1986

Determination of the vacancy migration energy of aluminum by NMR

Terry William Gullion
College of William & Mary - Arts & Sciences

Gullion, Terry William

DETERMINATION OF THE VACANCY MIGRATION ENERGY OF ALUMINUM BY NMR

The College of William and Mary in Virginia PH.D. 1986

DETERMINATION OF THE VACANCY MIGRATION ENERGY OF ALUMINUM BY NMR

A Dissertation

Presented to

The Faculty of the Department of Physics

The College of William and Mary in Virginia

In Partial Fulfillment

Of the Requirements for the Degree of

Doctor of Philosophy

---

by

Terry William Gullion

1986

APPROVAL SHEET

This dissertation is submitted in partial fulfillment of the requirements for the degree of

Doctor of Philosophy

Terry William Gullion

Terry William Gullion

Approved, October 1986

Mark S. Conradi

Herbert O. Funsten

Gina L. Hoatson

Henry Krakauer

Kenneth G. Petzinger

Gary C. DeFotis
Chemistry

TABLE OF CONTENTS

ACKNOWLEDGMENTS		v
LIST OF TABLES		vi
LIST OF FIGURES		vii
ABSTRACT		ix
Chapter		Page
I.	INTRODUCTION	2
II.	THEORY AND BACKGROUND	9
2.1	Simple Diffusion	9
A.	The Process	9
B.	The Equilibrium Number of Vacancies in a Solid	11
C.	The Jump Frequency	12
D.	The Jump Rate	13
2.2	NMR Theory	14
A.	Basic NMR	15
B.	Concept of Dipolar Order	16
C.	Jeener-Broekaert Experiment	17
D.	Relaxation by Conduction Electrons in a Metal	22
E.	Diffusion Contribution to T_{1D}	24
F.	NMR Determination of E_d and E_m	26
2.3	The NMR and Diffusion Specifics of Aluminum	27
A.	NMR Aspects of Aluminum Metal	28
B.	Diffusion Studies of Pure Aluminum Metal	29
III.	EXPERIMENTAL APPARATUS	35
3.1	Magnet, Magnet Power Supply, and Field Stabilization	35
3.2	Probe	38

3.3 Spectrometer 40

3.4 Temperature Control, Pulse Heater, Temperature Measurement . . . 44

IV. RESULTS and DISCUSSION 49

4.1 Pulse Heating 49

4.2 Electric Quadrupole Interaction . 53

4.3 Equilibrium Data 54

4.4 T-jump Experiment 60

V. CONCLUSIONS 70

APPENDICES

A. Calculation of the Equilibrium Concentration of Vacancies . . 72

B. Temperature Change as a Function of Applied Field 74

C. Calculation of the Thermal Equilibration Time 76

D. The Recovery of Vacancies Toward Equilibration After a Sudden Change in Temperature . . . 78

REFERENCES 80

ACKNOWLEDGEMENTS

Special thanks go to my advisor and a wonderful teacher Mark Conradi. His advice and insight have made an enormous impact on this work and on my graduate education.

I also thank T. J. Rowland of the University of Illinois for important comments concerning this work and for providing a copy of C-Y. Sun's dissertation.

On the lighter side, I express my deepest appreciation for the friendship of Melinda Sullivan. Her companionship made my stay in Williamsburg most enjoyable. Also, many thanks go to Su-Huai Wei, Bassam Hitti, and Timothy Williams for their friendship.

Lastly, the staff and faculty of the physics department of The College of William and Mary are gratefully acknowledged; they have provided a truly warm atmosphere for study.

LIST OF TABLES

Table		page
1	The Activation Energy of Self Diffusion in Aluminum	31
2	The Vacancy Formation Energy . . .	32
3	The Vacancy Migration Energy . . .	34

LIST OF FIGURES

Figure		page
2.1	Illustration of monovacancy diffusion. Atom A has exchanged places with vacancy B.	10
2.2	A model illustrating the transfer of Zeeman order to dipolar order by the Jeener-Broekaert experiment. . .	19
3.1	Tuned LC circuit (a) and impedance matching circuit (b). Fine tuning is done by adjusting C_T, C_C, and L'. .	39
3.2	Block diagram of the spectrometer. .	41
3.3	Modified duplexer.	45
3.4	Illustration of the 4-lead resistance measurement and the sample-coil geometry. The sample is folded about the dashed line and centered in the coil. . .	47
4.1	H_1 homogeneity of the sample coil. .	52
4.2	Equilibrium T_{1D} and $\tau_j/2(1-p)$ data. The solid line for the T_{1D} data is an eye guide. The line for the jump time data is the best fit and yields E_d=1.33 ev. The dashed line is T_{1e} as determined by $T_{1e}T$=1.802 sec K.	56
4.3	T_{1e} pulse sequence.	57
4.4	Pulse sequence for the T-jump experiment. The last three pulses are the Jeener-Broekaert experiment.	61
4.5	T-jump data with T_j=526 K. The line is the best fit and gives E_m=.71 ev. .	63
4.6	T-jump data with T_j=542 K. The line is the best fit and gives E_m=.66 ev. .	64

4.7 Illustration of the temperature response of the sample during the T-jump experiment. The heating pulse is applied during the first 80 msec. The decay time of the temperature is approximately 40 msec. . 68

ABSTRACT

Monovacancy diffusion is a thermally activated process characterized by an activation energy E_d. The diffusion of atoms requires the formation and migration of vacancies. The concentration of vacancies n/N is given by $n/N \approx \exp\{-E_f/kT\}$. It can be shown that the activation energy E_d is the sum of the energy to form a vacancy E_f and the energy required for an atomic jump E_m: $E_d = E_f + E_m$. Furthermore, the atomic jump rate ω_j can be shown to be thermally activated and given by $\omega_j \approx \nu_o (n/N) \exp\{-E_m/kT\}$ (ν_o is the attempt frequency).

NMR offers many techniques to measure the activation energy, E_d. However, there are no NMR techniques available for the determination of the migration energy. This thesis presents an NMR experiment for the measurement of the migration energy. It is a simple NMR experiment performed on a sample prepared with a nonequilibrium concentration of vacancies. By preparing the sample such that the vacancy concentration does not change with temperature, the jump rate has only one thermally activated term. Thus, the jump rate now has an activation energy equal to the migration energy E_m.

This experiment was performed on pure aluminum metal. The migration energy was found to be .69 ev ± 20% (the accepted value is .67 ev); however, we do not consider this an accurate determination. We do consider the experiment successful and promising. The activation energy of self diffusion was also determined; its value is 1.33 ev.

DETERMINATION OF THE VACANCY MIGRATION ENERGY OF ALUMINUM BY NMR

Chapter I

INTRODUCTION

There are many dynamical processes occurring within any solid; naturally these activities give the solid its unique characteristics. Simple diffusion by a mono-vacancy mechanism is the process of concern in this thesis; this is characterized by the movement of atoms (or molecules) through the solid by the jumping of an atom from one lattice site to a neighboring vacant lattice site (Pet68).

Thermodynamical arguments give a fairly simple equation governing the process of simple diffusion (Mot64). All solids contain an equilibrium number of vacancies n that depends on the temperature of the sample by

$$n=Nexp\{-E_f/kT\} \qquad (1.1)$$

where N is the number of lattice sites, E_f is the formation energy, k is Boltzmann's constant, and T is the temperature. The formation energy is the energy necessary to form a vacancy and is approximately equal to the difference in energy between an atom inside the crystal and an atom on the surface of the crystal. A

vacant lattice site and a neighboring occupied lattice site are separated by a potential barrier; the energy required for an atom to cross this barrier is the migration energy: E_m. An atom will have this energy a fraction of the time as dictated by the Boltzmann factor: $\exp\{-E_m/kT\}$ (Rei65). The number of jumps per second ω_j an atom makes is equal to the number of times it strikes the barrier separating the two sites times the probability it has the requisite energy times the probability that the neighboring site is vacant. That is

$$\omega_j=\nu_o\exp\{-E_m/kT\}\exp\{-E_f/kT\}. \qquad (1.2)$$

ν_o is the number of times per second the atom strikes the barrier and is commonly called the attempt frequency; its magnitude is the same as the Debye frequency. Equation 1.2 can be written as a single exponential with the definition $E_d=E_m+E_f$; E_d is called the activation energy of diffusion. The important point is that the jump rate is a thermally activated process and has been verified as such in a wide range of materials.

There are a handful of techniques commonly used to measure the activation energy. Radiotracer studies were among the first and are still widely used (provided a suitable isotope exists) (She79). In this method the sample is placed onto a slab of similar material doped with a radioactive isotope. Over time, the radioactive

isotope diffuses into the sample. The sample is then sectioned and the activity of each part is measured. Since the activity is proportional to the amount of the radioactive isotope present, the diffusivity can be determined which in turn yields the jump rate. This experiment is done as a function of temperature and thus yields the activation energy. There are numerous nuclear magnetic resonance (NMR) experiments used to determine the jump rate. These include line narrowing, T_1, spin echo, and stimulated echo experiments as well as ultralow field techniques such as $T_{1\rho}$ and T_{1D} experiments (Abr83, Ail71, Fuk81, Jee67, Sli64, Sli80). Line narrowing studies are useful when the jump time τ_j satisfies the condition $\tau_j \Delta\omega_{RL} \ll 1$. $\Delta\omega_{RL}$ is the rigid lattice line width. In the rigid lattice each nucleus experiences a local magnetic field; in general there will be a distribution of local fields. The spin-spin relaxation time T_2 is determined by this distribution. When diffusion becomes important then each atom experiences an average local field that will be less than the its local field in the rigid lattice. The result is that T_2 becomes longer and, accordingly, the line width becomes more narrow. A study of this narrowing as a function of temperature will yield the activation energy. It is well known in NMR theory that motions occurring with a rate near the Larmor frequency will

cause the occurrence of a T_1 minimum. Provided that the diffusion rate dominates the spin-lattice relaxation time T_1, a study of the minimum as a function of temperature and magnetic field yields the activation energy. Unfortunately, this technique is limited to relatively high temperatures. The area of spin echoes and stimulated echoes has seen much use in diffusion studies (see for example Liu84, Gul85). Only spins that never make a jump contribute to a spin echo; however, only jump times shorter than the rigid lattice T_2 can be measured. Stimulated echoes can measure jump times longer than measured by spin echoes since the spins spend the majority of their time parallel to the Zeeman field. In fact, jump times as long as T_1 can be measured by stimulated echoes. The ultralow field experiments (Sli64, Jee67) are similar to the T_1 experiment. The difference is that the effective field experienced by the spins during the experiment is greatly reduced and spatially random. Instead of fields of the order of several kilogauss, the effective field is only a few gauss. Thus the relaxation times $T_{1\rho}$ and T_{1D} are sensitive to motions in the kilohertz region which allows the study of diffusion to occur at more modest temperatures.

There also exists a wide variety of experiments capable of measuring the vacancy formation energy.

Quenching experiments have found much use in determining the formation energy in metals (Fed65). This experiment consists of preparing a specimen at a high temperature and then rapidly quenching it at a much lower temperature. This process freezes in the number of vacancies that existed at the high temperature. The electrical resistivity is immediately measured; there is a component of resistivity proportional to the number of defects frozen in by the quench. Measurement of the residual electrical resistivity as a function of the high starting temperature yields the formation energy. Thermal expansion experiments have also been used frequently to determine the formation energy (Sim60a). This experiment compares the relative change of the length of the sample to the relative change in its atomic spacing (determined by x-ray spectroscopy) as a function of temperature. These two are not the same since the concentration of vacancies is temperature dependent and comparison of the two parameters yields the concentration of vacancies as a function of temperature which in turn yields the formation energy. Positron annihilation studies has received more attention recently as a tool for determining the formation energy (Hau79, Wes79). Very simply put, the ratio of trapped and free positrons yields the concentration of defects. The temperature dependence of this ratio

yields the formation energy.

There are, by far, fewer techniques available for the measurement of the migration energy. Quenching experiments are used in metals (Fed65). The sample is quenched from a high temperature to a very low temperature (typically 77 K). Next the sample is raised to an intermediate temperature, called the annealing temperature, for a given amount of time and then returned to the low temperature where its resistivity is measured. The rate of annealing as a function of annealing temperature yields the migration energy. Neutron irradiation experiments are also used to determine the migration energy. They are quite similar to the quenching experiments except that neutrons instead of quenching from a high temperature are used to generate an excess vacancy concentration (Cer63).

As can be seen from the above introduction there is an abundance of NMR experiments to measure the activation energy. However, there are none for the measurement of the formation and migration energies. The existing techniques for the measurement of the formation and migration energy are mostly applicable to metals. Since NMR can be used to study practically any material, it would be useful to have an NMR technique capable of measuring the migration or the formation energy. This thesis discusses an NMR experiment capable of measuring

the migration energy. This experiment is an addition to the class of condition-jump NMR experiments (Gul84). As an example, the experiment is demonstrated on pure aluminum metal. After much of this work was completed, I was informed of an unpublished work by C-Y. Sun in which he too measured the migration energy of aluminum metal by a technique similar to the one presented here (Sun71).

Chapter II

THEORY AND BACKGROUND

Monovacancy diffusion is the physical process of interest here. In this chapter, the theory of the mechanism is given. A brief introduction to the theory of the Jeener-Broekaert experiment for the measurement of slow processes is also presented. Finally, an overview of relevant data concerning diffusion in aluminum metal is given.

2.1 SIMPLE DIFFUSION

A. The Process

The physical process of concern is the movement of atoms throughout the solid by a vacancy mechanism. Only diffusion by monovacancies will be considered here since this is the dominant diffusion mechanism in aluminum (Sim60a). Divacancies become noticeable in pure aluminum only near the melting point (Sim60a). Figure 2.1 illustrates the process. Atom A is located at a lattice site; all of the neighboring sites, except one, are occupied by the same type of atom. The vacant site is called a vacancy; the vacancy is labelled B in the

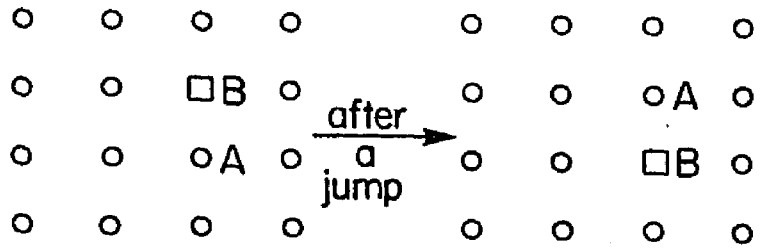

Figure 2.1: Illustration of monovacancy diffusion. Atom A has exchanged places with vacancy B.

figure. Atom A is vibrating in its potential well and strikes the potential barrier separating its lattice site and the vacant lattice site ν_o times per second. Typically ν_o is 10^{13} sec^{-1}. Due to thermal fluctuations, atom A will at some point in time have enough energy to overcome the barrier; the result is the vacancy and atom A have exchanged places. Of course, this process continues indefinitely.

B. The Equilibrium Number of Vacancies in a Solid

The idea of a perfect solid is an idealization that never occurs. Thermodynamics shows that a solid at equilibrium will have defects, the simplest defect being the common vacancy.

The thermodynamical state function of choice when dealing with solids is the Gibbs function. This arises because temperature and pressure are the intensive variables and the number of particles is the extensive variable. The Gibbs function is defined as

$$G=E+PV-TS \qquad (2.1)$$

where E is the internal energy, P is the pressure, V is the volume, T is the absolute temperature, and S is the entropy. At pressures of the order of one atmosphere the PV term may be neglected since it is much less than E. Thus, Eq. 2.1 becomes

$$G=E-TS. \qquad (2.2)$$

Often, G is called the free energy.

Consider the difference in free energy, ΔG, between a solid with n vacancies and one with no vacancies;

$$\Delta G = -nE_f - TS_f \qquad (2.3)$$

where E_f is the energy required to form a single vacancy and S_f is the difference in the entropy of the two solids. Recall that the entropy is proportional to the logarithm of the number of energetically equivalent states. A theorem states that $(\Delta G)_{T,P} > 0$ for any variation away from equilibrium at constant temperature and pressure; this implies the free energy must be a minimum for equilibrium (Van66). Minimization of ΔG with respect to the number of vacancies yields the equilibrium number of vacancies. The result is

$$n = N\exp(-E_f/kT) \qquad (2.4)$$

where k is Boltzmann's constant and N is the number of atoms. Equation 2.4 is derived in Appendix A. The strong temperature dependence of the vacancy concentration is important. Typically, E_f is of the order of 1 ev; this gives vacancy concentrations n/N of about 10^{-17} at room temperature for aluminum and about 10^{-3} near the melt. A good review of the above arguments is given in the book by Mott and Gurney (Mot64).

C. The Jump Frequency

As mentioned earlier, the atom vibrates about its

lattice point ν_o times per second. Put another way, the atom strikes the potential barrier separating it from the adjacent vacant site ν_o times per second. ν_o is often called the attempt frequency and is taken to be the Debye frequency. Usually, the atom lacks sufficient energy to overcome the barrier; but, on occasion it does have enough energy and an atomic jump occurs.

The energy needed to overcome the barrier is called the migration energy: E_m. The atom will have sufficient thermal energy to overcome the barrier a fraction $\exp(-E_m/kT)$ of the time. The jump frequency, p_j, is equal to the number of times the atom strikes the barrier times the probability it has enough energy to overcome the barrier:

$$p_j=\nu_o\exp(-E_m/kT). \qquad (2.5)$$

Thus, the jump frequency is thermally activated.

D. The Jump Rate

Two events must occur before an atom can jump into a vacant lattice site. First, the adjacent site must be vacant. Second, the atom must have the requisite energy to overcome the barrier.

The jump rate, ω_j, of atomic diffusion is the jump frequency times the probability the neighboring site is vacant. Since there are n vacancies and N lattice site, the probability each site is vacant is n/N. Thus, the

jump rate is

$$\omega_j=\nu_o\exp(-E_m/kT)\exp(-E_f/kT)=\nu_o\exp(-E_d/kT) \qquad (2.6)$$

where $E_d=E_m+E_f$ and is called the activation energy of diffusion. If there are Z nearest neighbors, the prefactor must be multiplied by Z; but, there already exists uncertainty in the prefactor. There are two additional entropic factors that appear in the prefactor that have not been considered. One of these is the additional entropy (S_m) that arises because of the movement of the atom over the saddle point of the potential barrier. The other entropy term (S_f) arises because the atoms surrounding a vacancy tend to relax about the vacant site, changing the local vibrational frequencies. In any event, the jump rate has two thermally activated terms; diffusion is a thermally activated process.

2.2 NMR THEORY

Nuclear magnetic resonance (NMR) has a rich history in the study of motions in solids and liquids. In fact, one of the first applications of NMR was the determination of diffusion coefficients in liquids (Hah50). The development of NMR slow motion techniques has made the study of diffusion in solids an everyday occurrence (Sli64, Jee67).

A. Basic NMR

The interaction of interest is the coupling of a magnetic field with the nuclear magnetic moment. The Hamiltonian of a nucleus with nuclear magnetic moment $\vec{u}$ in a static field $\vec{H}_o$ is

$$H=-\vec{u}\cdot\vec{H}_o. \qquad (2.6)$$

The eigenvalues of this Hamiltonian are

$$E_m=-\gamma\hbar H_o m \qquad (2.7)$$

where $m=I,I-1,....-I$, γ is the nuclear gyromagnetic ratio, I is the nuclear spin quantum number, and $\hbar$ is Planck's constant divided by 2π. There are (2I+1) equally spaced energy levels; the difference in energy between adjacent levels is $-\gamma\hbar H_o$. If the spins are in thermal equilibrium, then the energy states are occupied according to the Boltzmann factor; that is, the probability p_m that a given spin has energy E_m (not to be confused with the migration energy) is $p_m=\exp(-\gamma\hbar H_o m/kT)$. Any spin system that occupies its energy levels according to the Boltzmann factor is said to be described by a temperature T (Abr83, Sli80). This temperature may or may not equal the bath temperature. In solids, the most obvious bath is the lattice and the temperature of the lattice and spin system will eventually become equal if there is a coupling between the two systems. The net magnetization of the nuclear spins obeys Curie's Law

$$\vec{M}=C\vec{H}_o/T \qquad (2.8)$$

where C is a constant equal to $N\gamma^2\hbar^2I(I+1)/k$ and N is the number of spins.

The magnetization is not achieved instantaneously but appears at a rate $1/T_1$. T_1 is called the spin-lattice relaxation time. This rate is controlled by mechanisms which allow the transfer of energy between the spin system and the lattice. T_1^{-1} is strongly dependent upon motions occurring with frequencies near the Larmor frequency (Blo48). The Larmor frequency is γ times the magnetic field strength.

B. Concept of Dipolar Order

Consider a solid which has been allowed to soak in a static magnetic field and has acquired a magnetization $\vec{M}$. If the sample is removed from the magnetic field, it will have zero magnetization according to experimental observation. If the removal was done adiabatically and the sample is adiabatically reintroduced to the magnetic field with the constraint that the total time of the procedure is less than T_1, a remarkable event is observed. The magnetization reappears (without waiting T_1 again)!

This phenomenon can be understood. Since the experiment was done adiabatically then it was an isentropic process. The Zeeman order was transferred

to dipolar order when the sample was removed from the magnetic field. Dipolar order is the preferential alignment of the nuclear spins along their local magnetic fields. These local fields are created by neighboring nuclear magnetic moments. Since the local fields are random throughout the solid then this explains why no magnetization was observed while the sample was out of the applied field. When the sample is isentropically reintroduced to the field, the dipolar order is adiabatically transferred to Zeeman order and the magnetization reappears in a time short compared to T_1 (Fuk81).

C. Jeener-Broekaert Experiment

There are several easy ways to transfer Zeeman order into dipolar order. The method mentioned above is the first to come to mind. A similar technique is to reduce the applied field strength adiabatically to zero. These techniques are fine provided T_1 is long or provided the experimenter has the patience to undertake these methods. Fortunately, several pulse techniques have been developed to transfer Zeeman order into dipolar order in the rotating frame; these include the adiabatic demagnetization in the rotating frame (And62) and the Jeener-Broekaert three pulse technique (Jee67). The Jeener-Broekaert experiment is used here.

A simple model describing the way the three pulse experiment transfers Zeeman order into dipolar order is given (Jee67). The model is flawed but offers an easy visualization of how the transfer is accomplished. Fig. 2.2 illustrates the idea and is the same used in the original work of Jeener and Broekaert.

First, consider the radiofrequency carrier to be in the center of the line; this results in fast spins on one side of the carrier and slow spins on the other side. The average spins will be on the carrier. Fast in this context implies that these spins have a local magnetic field component parallel to the Zeeman field and slow implies that these spins have a local magnetic field anti-parallel to the Zeeman field.

Second, consider the 90_x-t-90_y pulse sequence. Prior to the first pulse the sample is magnetized (Zeeman order): there is an abundance of fast, slow, and average spins parallel to $\vec{H}_o$ ($\vec{H}_o$ defines the z-axis). Immediately after the first pulse, these spins are aligned along the -y-axis. During the waiting time t the spins begin to dephase; the fast spins travel counterclockwise in the x-y plane, the slow spins travel clockwise, and the average spins remain parallel to the -y-axis. The time t is chosen such that the average fast spins and the average slow spins precess approximately + or - 90^o. After the second pulse is applied

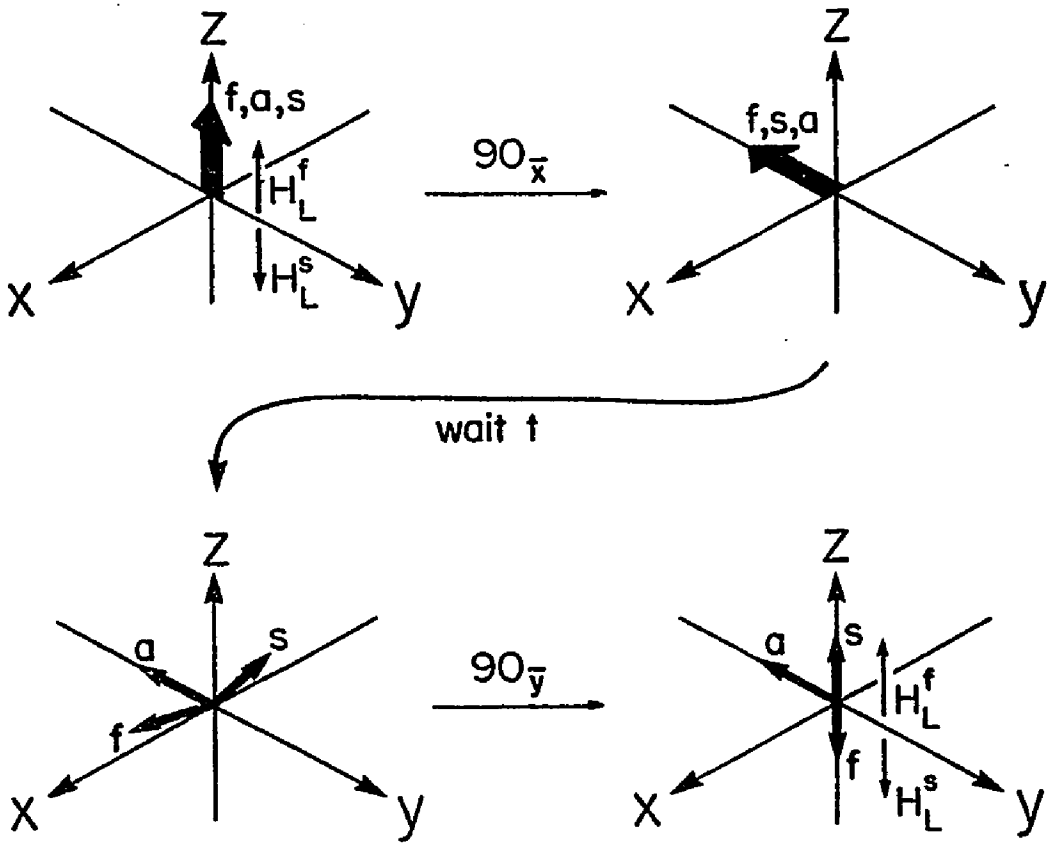

Figure 2.2: A model illustrating the transfer of Zeeman order to dipolar order by the Jeener-Broekaert experiment.

the slow spins are parallel with the z-axis and the fast spins are anti-parallel to the z-axis. Thus the fast spins are found to be anti-parallel to their local fields (parallel to +z axis) and the slow spins are anti-parallel to their corresponding local field (anti-parallel to the + z axis). The resultant energy is the sum of the energy of the fast spins and slow spins; this energy is of the form $E^{total} \approx -2\gamma\hbar H_L$. This corresponds to dipolar order. More evidence supporting this hypothesis is that the bulk magnetization is zero but the magnetization along the local fields has the same magnitude and has only changed direction.

As mentioned earlier, this explanation of the Jeener-Broekaert pulse sequence does have problems. A major flaw is that the finite pulses do not preserve the fast or slow character of the spins. This occurs because the local fields are due to the neighboring spins; these spins change orientation when the pulses are applied and thus a change in the local fields arise. Another problem with this model is it ignores the flip-flop terms in the dipolar Hamiltonian: terms like $I_{+1}I_{-2}$. Flip-flops may occur in the time interval t (roughly one per spin in time T_2); thus the z-component of the local field changes for those nuclei which have undergone this process. This is contrary to the above model where it was assumed that the local field

never changed during the experiment. Thus, it becomes obvious that the model ignores many important processes. Still, this model does make the three pulse method understandable.

Jeener and Broekaert used spin thermodynamics and the density matrix to prove their technique. Their results indicate that in a system with purely dipolar coupling and a Gaussian line shape only 52% of the available Zeeman order can be transferred into dipolar order (the actual efficiency depends on the lattice). In order to achieve this efficiency, the first pulse must be a 90 degree pulse and the second pulse must be a 45 degree pulse; the phase shift between the two pulses must be 90 degrees. The time between the two pulses must be near T_2. Furthermore, the technique is applicable only when $T_1 \gg T_2$, where T_2 is the spin-spin relaxation time.

The big question is: Why transfer Zeeman order into dipolar order? Immediately after the transfer, the alignment of spins along their local fields (dipolar order) is much larger than allowed by Curie's Law at thermal equilibrium. The dipolar order must relax to the equilibrium value which is nearly zero since the local field is small. The relaxation is exponential and has a time constant T_{1D}. T_{1D} is called the dipolar relaxation time. Just as T_1 is sensitive to motions

occurring at the Larmor frequency, T_{1D} is sensitive to motions occurring at the Larmor frequency of the local field. Typically, these motions are in the kilohertz region. A different but equivalent view: if an atom makes a jump to a new site then it experiences a new local field. This results in relaxation of the dipolar order (see below). Thus, very slow motions and atomic jumping can be detected by monitoring the dipolar relaxation time (Ail71).

D. Relaxation by Conduction Electrons in a Metal

One of the dominant spin-lattice relaxation mechanisms in a metal is due to the conduction electrons (Sli80). In a relaxation process the nucleus undergoes a transition which results in the absorption or emission of energy. Since energy is conserved there must exist a system capable of exchanging energy with the spin system. The conduction electrons form such a system. A simple explanation is provided by the $\vec{I}\cdot\vec{S}$ contact interaction; I is the nuclear spin and S is the electron spin. This interaction has terms like I_zS_z (this term is not important to relaxation but is responsible for the Knight shift) and $I_+S_-+I_-S_+$. Whenever a nuclear spin makes a transition, an electron undergoes a simultaneous transition. The electron goes from an

initial state described by wave vector k and spin orientation s to a final state described by a wave vector k' and spin orientation s'. The energy difference between the two electron states is equal to the difference in energy between the initial and final states of the nuclear spin. This process is a result of the flip-flop term of the contact interaction.

Korringa derived an expression for the spin-lattice relaxation time due to the conduction electrons in a metal (Kor50). The expression was derived by considering the coupling between the s-state electrons (these electrons' wavefunction are nonvanishing at the nucleus) and the nuclei. The spin-lattice relaxation time due to the conduction electrons is T_{1e} and satisfies

$$T_{1e}(\Delta H/H)^2=(\hbar/4\pi kT)(\gamma_e/\gamma_n)^2. \qquad (2.9)$$

$\Delta H/H$ is the Knight Shift; the resonance frequency in a metal is usually higher than in a diamagnetic compound containing the metal. This arises because of the I_zS_z term in the contact interaction between the electrons and the nuclei (Kni56).

There are two important properties of this relation. First, T_{1e} is proportional to 1/kT. Nuclear transitions involve small amounts of energy; only electrons with empty adjacent states can participate in the transfer of energy. In a metal, these particular

electrons are those in the tail of the fermi distribution; the number of electrons in the tail is proportional to kT. Since the relaxation rate is proportional to the number of participating electrons, then T_{1e} is proportional to 1/kT. Second, $T_{1e}T$ is independent of the magnetic field strength because the nuclear spin frequencies are small compared to relevant energies, like kT.

Equation 2.9 was derived for spin-lattice relaxation. However, since it is independent of the magnetic field strength, it is applicable to relaxation along the local fields with one exception. The relaxation rate along the local fields is twice that of high-field spin-lattice relaxation; that is

$$T_{1D}=(1/2)T_{1e}. \qquad (2.10)$$

The factor of 2 arises because Zeeman energy involves only one nuclear spin whereas the dipolar energy is relaxed if either of the pair makes a transition. In principle, the proportionality factor may be different from 1/2 since there may exist correlations between electrons on adjacent lattice sites (And59).

E. Diffusion Contribution to T_{1D}

There is usually a temperature regime in most materials where atomic diffusion occurs at a rate that will be important in relaxation.

The dipolar relaxation time is determined by processes occurring in the kilohertz region. Slow atomic motions are important in determining T_{1D}. The strong collision theory of Slichter and Ailion (Sli64) considered the effects of slow atomic jumps on the dipolar relaxation time. Their assumptions were that the time between jumps is much greater than T_2 and that the sudden approximation holds. The first assumption allows the establishment of a spin temperature after each jump. The second assumption implies that the spin orientation does not change during a jump (a jump occurs in a time of 10^{-13} seconds, a time much faster than the time required for a spin to make a single precession) but does result in a drastic change of the dipolar Hamiltonian.

This theory showed that the dipolar relaxation rate is proportional to the jump rate:

$$1/T_{1D}=2(1-p)/\tau_j. \qquad (2.11)$$

τ_j is the time between jumps. Whenever a jump occurs, the diffusing atom will most likely acquire a new local field much different from its original local field (the local fields are nearly random in space) and at the same time its spin orientation will be the same after the jump as before the jump. The diffusing atom's original partner also experiences a change in local field. Thus, both atoms are involved in relaxing the dipolar order

and the relaxation rate of the dipolar order is twice the jump rate. However, since the local field of the atoms after the jump is not completely random relative to their local fields before the jump, there is a correction to the relaxation rate. This correction is the (1-p) factor and comes about by the fact that each atom is coupled to a varying degree to more than one neighbor.

F. NMR Determination of E_d and E_m

NMR offers a means to determine the activation energy of diffusion and the migration energy of diffusion. The measurement of the dipolar relaxation rate allows the determination of the jump rate. The relaxation rate due to the conduction electrons and the relaxation rate due to diffusion are assumed to add to produce the overall dipolar relaxation rate in a metal:

$$1/T_{1D}=2(1-p)/\tau_j+2/T_{1e}. \qquad (2.12)$$

The activation energy can be determined by measuring the jump rate as a function of temperature. This requires measuring T_{1D} by the Jeener-Broekaert experiment and the measurement of the spin-lattice relaxation rate by conventional NMR techniques.

The migration energy is slightly more difficult to obtain. Recall that the jump rate ω_j satisfies Eq. 2.6 and is proportional to the number of vacancies:

$$\omega_j(T)=\nu_o[n(T)/N]\exp(-E_m/kT). \qquad (2.13)$$

The method for the measurement of the migration energy is as follows. First, prepare the sample at equilibrium at temperature T_s; the number of vacancies is $n(T_s)$. Second, change the temperature rapidly to temperature T_f. The vacancy concentration will change slowly as a result of the temperature change. Since vacancies are created and destroyed at dislocations, there is a finite time required for the change in their concentration to occur. By making the change in temperature fast enough to insure that the vacancy concentration does not change, then $n(T_f)=n(T_s)$ is obtained. Third, immediately after the temperature change, measure T_{1D}. This yields a jump rate $\omega_j'(T_f)$. This jump rate satisfies

$$\omega_j'(T_f)=\nu_o[n(T_s)/N]\exp(-E_m/kT_f). \qquad (2.14)$$

Thus, a measurement of ω_j' as a function of T_f yields the migration energy alone.

2.3 The NMR and Diffusion Specifics of Aluminum

There are two isotopes of aluminum: ^{26}Al and ^{27}Al. This is interesting in that only ^{27}Al occurs naturally; ^{26}Al can be manufactured (with extreme difficulty) and is the only one that is radioactive. It is for this reason that tracer studies were late in determining the diffusion parameters of aluminum. Of concern here is ^{27}Al. This isotope has spin I=5/2 and a gyromagnetic

ratio equal to $2\pi x11.1x10^2$ (sec oersted)$^{-1}$. As allowed by its spin (>1/2), it also has a quadrupole moment $Q=.156x10^{-24}$ cm^2.

Pure aluminum metal has a melting point near 660 ^oC. Its structure is face centered cubic.

A. NMR Aspects of Aluminum Metal

The cubic symmetry of aluminum metal is important from an NMR viewpoint. Since the spin is 5/2, the nucleus has an electric quadrupole moment (Sli80). This moment interacts with electric field gradients and produces a broader resonance; more importantly, since the energy levels will not be equally spaced then the relaxation will not be exponential and a unique T_1 will not exist. However, the cubic symmetry of the crystal results in the lack of electric field gradients near the nucleus. If the crystalline symmetry is broken, then the electric quadrupole becomes important. One possible means of destroying the symmetry is the addition of defects such as vacancies. As will be seen, the temperature region of this work has such a low concentration of vacancies that no noticeable effects due to the quadrupole moment arise. Indeed, the early NMR work of Spokas and Slichter showed the quadrupole moment to become noticeable only at temperatures above 450 ^oC (Spo59).

The nature of the types of defects present in aluminum is important. The work of Simmons and Balluffi gave considerable insight into this problem. They compared the expansion of the lattice parameter with bulk expansion measurements and found that the dominant defects are vacancy type defects, all other defects being negligible.

There are only two spin relaxation mechanisms that are important in this work. First, there is the interaction of the nuclear spin with the conduction electrons. The spin-lattice relaxation time satisfies the Korringa relation with $T_{1e}T \approx 1.8$ sec K. This holds over the temperature range 1 ^{o}K to the melting point (Spo59). The conduction electrons are also extremely important in determining the dipolar relaxation rate. Second, there is the magnetic interaction between nuclear spins. Since each spin has a magnetic moment, each spin will experience a magnetic field due to its neighboring spins. An atomic jump will change the local field of the atom that makes the jump and the local fields of its neighbors. This results in a change in the dipolar energy of the system and thus will be important in determining the dipolar relaxation rate.

B. Diffusion Studies of Pure Aluminum

Diffusion has been studied intensively in aluminum by

many people. Tables 1, 2, and 3 present some of the data obtained by these researchers. First, Table 1 presents the activation energy of diffusion. Several methods we re employed and all are in reasonable agreement. Amazingly, the results from the tracer experiments are slightly higher than the other results; this is important since this is the only method that measures diffusion directly. Since the half-life of ^{26}Al is so very long, the tracer measurements are difficult and not as accurate as would be expected for an isotope with a shorter half-life. The range of E_d is from 1.25 to 1.5 ev with 1.33 ev as the generally accepted value. Second, Table 2 presents the formation energy data. Once again, many techniques were employed. The quenching and dilatation data produce a formation energy of .76 ev whereas the positron annihilation data yield a value closer to .66 ev. This discrepancy has been analyzed by Seeger (See73). He notes that the dilatation experiments failed to consider the effects of divacancies near the melt which resulted in an overestimation of the formation energy. His analysis of the dilatation experiments produced a formation energy of .66 ev which is in excellent agreement with the positron annihilation studies. The problems with the quenching data has been discussed by Takamura (Tak65). He (and others) notes that thick samples have different cooling

TABLE 1

THE ACTIVATION ENERGY OF SELF DIFFUSION IN ALUMINUM

METHOD	E_d (ev)	REFERENCE
NMR linewidth	1.32	Sto65
NMR T_2	1.4	Spo59
NMR $T_{1\rho}$	1.25	Fra67
NMR $T_{1\rho}$	1.32	Sun71
Tracer	1.48	Lun62
Tracer	1.48	Bey68
Quenching	1.3	Pan58
Quenching	1.44	DeS59a
Quenching	1.33	Fed59

TABLE 2

THE VACANCY FORMATION ENERGY

METHOD	E_f (ev)	REFERENCE
Quenching	.77	Kab65
Quenching	.76	Duc66
Quenching	.79	DeS59a
Quenching	.70	Fur76
Quenching	.69	Tza76
Resistivity	.77	Sim60b
Thermoelectric power	.74	Bou68
Dilatation	.77	Fed58
Dilatation	.76	Sim60a
Dilatation	.71	Bia66
Positron annihilation	.62	Sne72
Positron annihilation	.66	McK72
Positron annihilation	.64	Hal74
Positron annihilation	.66	Tri75
Positron annihilation	.67	Kim74
Positron annihilation	.68	Dlu77
Positron annihilation	.66	Flu78

rates; since more time is needed to quench the sample then many of the defects have time to combine or to change character. This results in a sample with different characteristics than presumed and the resulting analysis is much more difficult. The most recent quenching experiments attempted to circumvent this problem. One (Fur76) paid particular attention to specimen thickness and analyzed the data accordingly; this gave a formation energy of .70 ev. Another experiment (Tza76) used extremely thin samples and performed the experiment at 200 ^{o}C (to minimize divacancy formation); this resulted in a value of .69 ev for the formation energy. These two results are noticeably lower than past quenching experiments. Thus, it appears that the formation energy of pure aluminum is .66 ev. Third, Table 3 presents the migration energy data. There is little data since there are few techniques capable of measuring the migration energy. Of course, the difference in the activation energy and the formation energy gives the migration energy. There is some scattering in the available data. The value obtained by using the values of the activation energy and the formation energy is .67 ev which is in reasonable agreement with the values in Table 3.

TABLE 3

VACANCY MIGRATION ENERGY

METHOD	E_m (ev)	REFERENCE
Quenching	.65	DeS59b
Quenching	.65	Has80
Neutron irradiation	.59	Cer63
NMR $T_{1\rho}$	.55	Sun71
Pulsed heating	.66	Ono78

Chapter III

EXPERIMENTAL APPARATUS

This chapter is concerned with the description of the apparatus and methods used throughout the experiment.

3.1 MAGNET, MAGNET POWER SUPPLY, AND FIELD STABILIZATION

A Varian model 3902 electromagnet was used in this experiment. It is an iron core, low impedance, water cooled magnet. The pole faces are 30.5 cm in diameter and are separated by 3.5 cm. The operating field throughout the experiment was approximately 19.3 kilogauss; this corresponds to a resonance frequency of approximately 21.638 Mhz for Al.

The magnet power supply is a water cooled, solid state instrument. This current regulated power supply has a bank of 59 pass transistors arranged in parallel mounted on a water cooled plate. These transistors are driven by passgate drivers. The passgate drivers and the pass transistors constitute the passgate circuit. Naturally, the current passing through the transistors depends on how hard the passgate drivers are driving the

transistors. In effect, the overall action is much like a variable resistor in series with the magnet coils.

Field stability is of utmost importance in the NMR of solids whenever signal averaging is performed. Our field was stable to better than 1 ppm. There are, of course, many ways to ensure a stable magnetic field. One method is to hire someone to constantly adjust the current to the magnet; however, there are much cheaper and much more dependable ways to ensure magnetic field stability. Three methods are used for field stabilization: current regulation, flux locking, and NMR field frequency locking.

Current regulation uses a sensing resistor to monitor the magnet current. The voltage across the sensing resistor is compared to a reference voltage. The difference (error voltage) in the two voltages is amplified and applied to the base of the passgate drivers. This forms a negative feedback loop resulting in the adjustment of the current passed by the power transistors and the magnetic field strength is corrected.

Rapid changes in the magnetic field are counteracted by a flux locker. Two sets of coils are used: the pickup and buckout coils. The pickup coils detect changes in the magnetic field according to Faraday's Law. This is amplified and a correction signal is then

sent to the buckout coils which create a magnetic field correction. Also, a correction signal is sent to the power supply; this alleviates the long term load on the buckout coils. However, very small or very slow changes in the magnetic field cannot be sensed by the pickup coils. This is because Faraday's Law is a derivative law; that is $\xi=-d\phi/dt$.

Initially, one would consider the current regulation and flux locking schemes to be adequate for field regulation. This, however, is not the case. Consider the effect of temperature change of the air or magnet cooling water; both would change the physical nature of the magnet and would thus change the magnetic field. Also, small changes in the magnetic field that occur over long periods of time cannot be detected by the flux locker. Neither of the two previous field regulation techniques would be able to deal with problems of this sort. So, a field regulation scheme which directly monitors the magnetic field is desirable; this is the NMR field-frequency locking method. The instrument used here has been thoroughly described in the thesis of Phil Kuhns (Kuh82). Briefly, it consists of a miniature NMR probe and cw spectrometer. The probe is a tuned LC circuit with doped C_6F_6 as a sample; the doping is done with the free radical TEMPO and is responsible for reducing the T_1 of the ^{19}F to approximately 20 milli-

seconds. The time averaged response of the ^{19}F NMR signal tells how far and in which direction the magnetic field has drifted. A correction signal is then sent to the flux locker where a correcting field is applied by the buckout coils.

3.2 PROBE

Figure 3.1 shows the tuned circuit and the impedance matching circuit used to transfer the rf from the transmitter to the probe. The tuned circuit is an LC circuit with fixed values; this has an impedance that is typically higher than the characteristic impedance of the spectrometer (50 ohms). The impedance matching circuit provides the means to match the impedance. The tuning and coupling capacitors are variable air plate capacitors; these offer the necessary flexibility to keep the circuit tuned and the impedance matched.

Several types of capacitors were tried in the tuned circuit. These included teflon trimmer, ceramic, and mica capacitors. During long rf pulses (80 msec), the air variable capacitors experienced rf breakdown. The ceramic capacitors were quite capable of sustaining the long rf pulses but these capacitors' capacitance drifted due to the temperature changes produced by heating from the long rf pulses. The inexpensive mica capacitors worked best even though they too experienced some

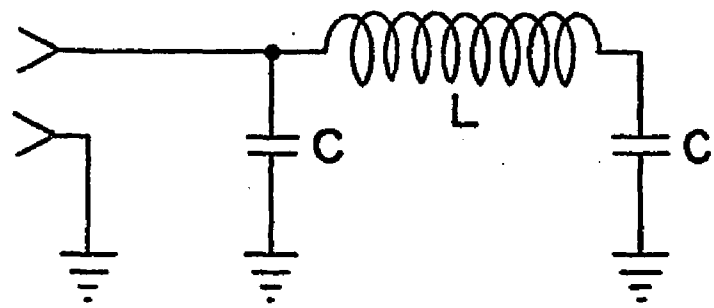

(a)

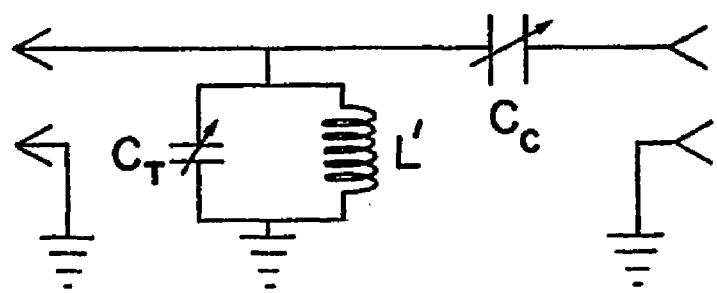

(b)

Figure 3.1: Tuned LC circuit (a) and impedance matching circuit (b). Fine tuning is done by adjusting C_T, C_C, and L'.

heating due to loss.

3.3 SPECTROMETER

The NMR spectrometer consists of three major units: the transmitter, the duplexer, and the receiver. It is a heterodyned, four-phase, pulsed unit. The gating and phasing are done at the intermediate frequency of 30 Mhz. Figure 3.2 is a block diagram of the spectrometer.

The first element of the transmitter is the General Radio Company type 1164A coherent frequency synthesizer. This was used to generate the 30 Mhz intermediate frequency and the 1 Mhz signal used by the NMR field-frequency locker. A tunable signal with frequency of 30 Mhz plus the NMR resonance frequency ν_o was also produced; this signal is later heterodyned down to the NMR frequency.

The power splitter takes the 30 Mhz signal and generates two 30 Mhz signals in phase with one another. The same is done to the $30+\nu_o$ Mhz signal.

The switchyard generates four 30 Mhz signals with different phases: 0^o, 90^o, 180^o, and 270^o. These signals are gated and then combined; the sum is then heterodyned to the frequency ν_o. This illustrates one advantage of heterodyning in that any phase of arbitrary ν_o signal can be produced without any modifications of

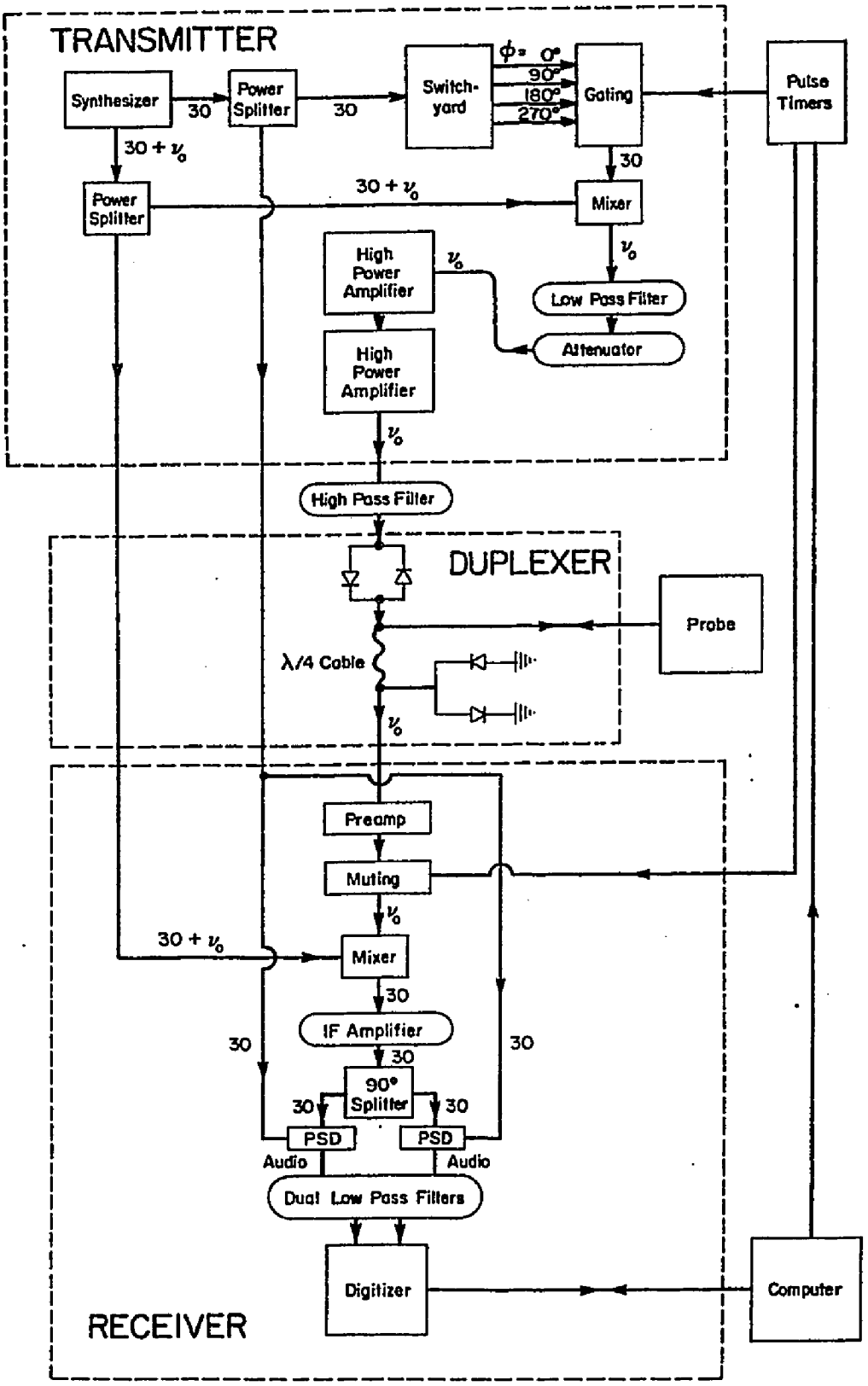

Figure 3.2: Block diagram of the spectrometer.

the pulse circuitry.

High frequency components will be generated during the process of heterodyning (sum and difference frequencies). Therefore, a low pass filter is inserted after the heterodyning circuit to eliminate these components.

The last stage of the transmitter consists of two high power amplifiers. The first amplifier is an ENI model A-300 amplifier; this is a 300 watt class A amplifier. This amplifier drives the second amplifier which is a modified Hallicrafters unit. The Hallicrafters is class C and uses RCA 7094 power tubes. In cascade, the two power amplifiers generated 1200 watts of power.

The last stage of the transmitter is followed by a high pass filter. This filter is used to filter out any low frequency components generated by the amplifiers.

The signal now enters the duplexer. The duplexer operates as a switchbox. The crossed diodes conduct during the time the amplifiers are on since the voltage is much higher than the 1.0 volt necessary to start conduction. When the amplifiers are off the diodes act as an infinite resistance and will not pass any signal from the probe (the signal from the probe is roughly 1.0 microvolt).

When the pulse from the amplifier passes through the crossed diodes, it has two paths it can go. The

quarter-wave cable and grounded crossed diodes have the property that it appears as an infinite impedance when the grounded crossed diodes conduct (Sen71); therefore, the only path available to the high power pulses is to the probe. When the nuclear signal from the probe reaches the junction containing the quarter-wave cable and crossed diodes, it must go in the direction of the preamplifier since the quarter-wave now appears to have low impedance. The signal cannot pass through either set of diodes since it is very weak.

The signal enters the receiver at the preamplifier. The preamplifier is a homemade device tuned at the NMR resonance frequency.

After the signal passes the preamplifier, it is heterodyned to the intermediate frequency of 30 Mhz. Then the signal is amplified and detected by phase sensitive detection. The phase sensitive detection results in two signals: one in phase and one in quadrature. The output signal is now in the audio range and is filtered by the low pass filters; this sets the receiver bandwidth and reduces the noise accordingly.

Since it is very difficult to store, average, and analyze an analog signal, the signal is digitized. This is done with a Biomation model 2805A digitizer. It digitizes 2048 points per channel. Of these, 1024 are sent to the computer where the data is stored and later

manipulated. The computer is also used for the initiation and timing of the pulse sequences used in the experiment.

3.4 TEMPERATURE CONTROL, PULSE HEATER, TEMPERATURE MEASUREMENT

The equilibrium temperature of the sample was controlled by a proportional mode, home-made temperature controller. This instrument works around a negative feedback loop and gates the 120 volt line voltage across the heating resistor. The heating resistor is nothing more than a coil of nichrome wire. Air was used as the heating gas. The background temperature was controlled to within a half of a degree over long periods of time.

Due to the nature of the experiment, the temperature of the sample must be raised by a fair amount and very rapidly; this is called T-jumping. This is done by rf heating. The rf is coupled to the aluminum sample using the same coil and tuned circuits that are used for the NMR experiments. However, a simple modification must be done to the duplexer in order to protect the crossed diodes. Since the crossed diodes cannot tolerate high currents over a long period of time (the rf heating pulse is 80 msec), they must be bypassed during the heating pulse. Figure 3.3 shows the modified duplexer. The modification consists of inserting a relay that operates in the following manner. When the

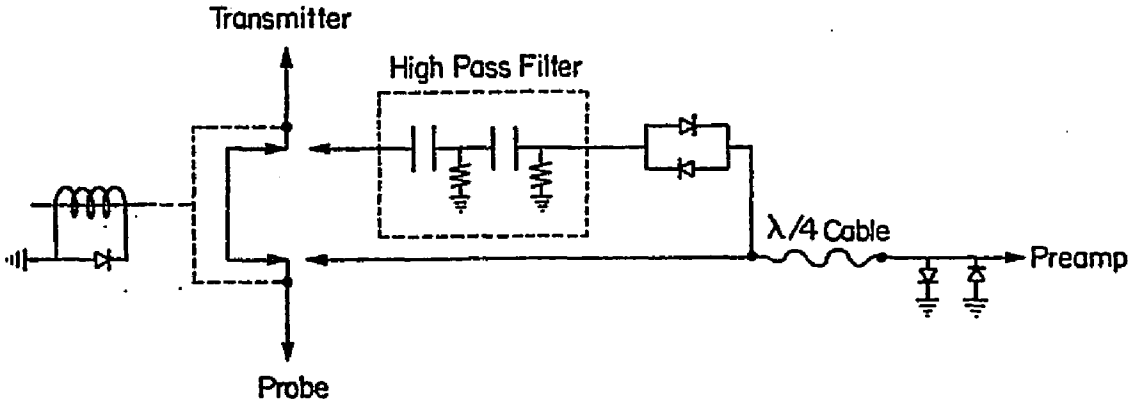

Figure 3.3: Modified duplexer.

rf heating pulse is applied, the rf goes directly from amplifier to the probe thereby isolating the high rf from the crossed diodes and the receiver. Immediately after the long pulse of rf, the relay connects the amplifier to the crossed diodes and the probe to the quarter-wave cable which is the normal operating mode for the NMR rig and is identical to Figure 3.2.

The magnitude of the temperature change was controlled by gating the duty cycle of the rf heating pulses in an on-off mode during the time set aside for heating; this time was 80 msec in all experiments. By controlling the width and time between pulses the temperature jump could be adjusted from 0 to approximately 100 K. However, since it takes 20 msec to close the relay and since the temperature decays to the background rather rapidly (estimated time constant of 40 msec), the maximum useful temperature jump was 50 K.

The temperature of the air surrounding the sample was measured with a copper-constantan thermocouple. Since the experiment was normally carried out at temperatures exceeding the melting point of tin-lead solder, the copper-constantan junction was silver soldered to insure good contact. A four-lead resistance technique was used to measure the temperature of the sample as a function of time; this is illustrated in Figure 3.4. The sample was constructed such that it had

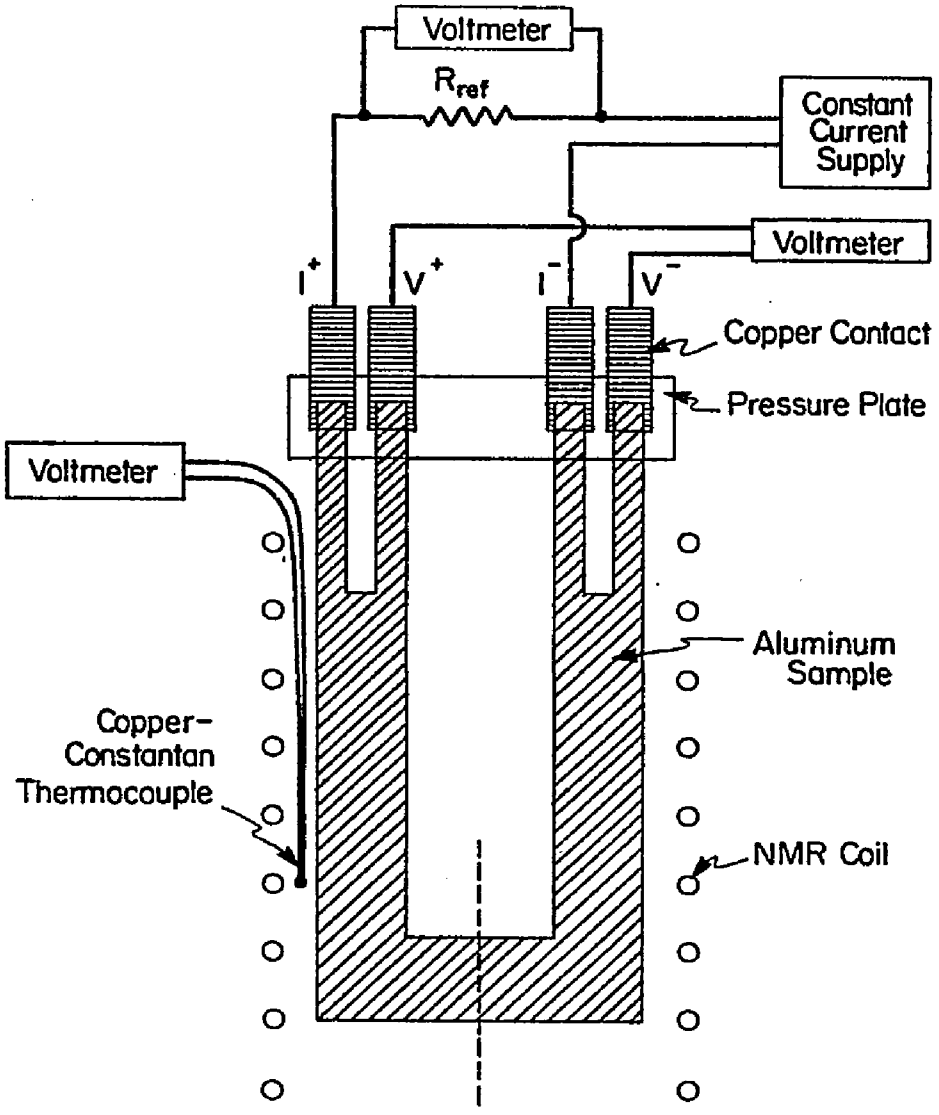

Figure 3.4: Illustration of the 4-lead resistance measurement and the sample-coil geometry. The sample is folded about the dashed line and centered in the coil.

four leads; these leads ran out the top of the NMR coil to four copper strips. Each of the aluminum leads was paired with one of the copper strips; these pairs were electrically insulated from one another by sheets of mica. The assembly was held together by two copper plates screwed together with much force which also guaranteed good electrical contact between the copper and aluminum leads. A strip of manganin wire with a resistance near that of the aluminum was used as a reference to insure that the current applied to the sample was the same for each measurement.

CHAPTER IV

RESULTS AND DISCUSSION

The results of the experiment are presented here. Also, recommendations are made that will, perhaps, improve the technique during its future applications.

4.1 PULSE HEATING

Since a four-lead resistance measurement was used for monitoring the sample temperature, there exists a question of temperature uniformity within the sample. After all, it is possible that small sections of the sample get extremely hot in comparison to other sections.

The sample was centered on the long axis of the NMR coil and held in place by one slab of mica. This arrangement ensures that the applied radiofrequency field H_1 is always parallel to the surface of the aluminum sample. Typically, the background temperature is approximately 530 K during the T-jump experiment. The T-jump is performed by the application of an intense rf field which results in joule heating of the sample as described in Appendix B. There it is shown that the

change in temperature obeys

$$\Delta T = B^2(\Delta t)/2c\sigma\rho d^2. \qquad (4.1)$$

The magnetic induction can be determined by noting that the time required to execute a 90° pulse is equal to $\pi/(\gamma B)$. This time was determined to be 2.8 microseconds; this results in a magnetic induction of 161 gauss. But this is not the number to be blindly plugged into the equation. Due to the long times required to get a sizeable heating (typically 80 msec), there is an enormous drain on the power supplies. In fact, a pulse length of a few milliseconds shows a substantial reduction of the applied voltage across the sample coil. Observation of this reduction for 80 millisecond pulses showed a 20% reduction in the applied voltage; thus, the magnetic induction value used for calculating the temperature change is 129 gauss. For a 70 millisecond pulse, Eq. 4.1 predicts a temperature change of 66 K; the observed temperature change was 63 K. This is fortuitously good agreement.

These numbers are in very good agreement yet there still exists some doubt as to the uniformity of the temperature jump as a function of position in the coil. That is, there is the question of H_1 homogeneity of the coil. The H_1 homogeneity was determined by measuring the 90° pulse time of a water sample doped with $FeCl_3$ as a function of position in the coil. The doping is for

convenience since this reduces the T_1 of water to the order of milliseconds. The length of the coil was 1.7 cm and the size of the water sample was 2 mm. 90° pulse times were measured at each increment of 1/4 cm. These times are shown as a function position in the coil in Figure 4.1. The length of the coil and the sample are superimposed on the plot. The distribution of 90° pulse times is within 5% of the average value. Thus, it is seen that the H_1 is relatively homogeneous.

One last question remains concerning the temperature of the sample. Since the heating occurs within the classical skin depth of the sample, there remains the question of temperature uniformity from the surface to the center of the sample. It is shown below that this is not a problem. In Appendix C is was shown that the time needed for two regions of the sample separated by a distance l and differing in temperature by ΔT to come to thermal equilibration is

$$t_T=(1.2\ \text{sec/cm}^2)l^2. \qquad (4.2)$$

The samples used had a thickness of .025 mm; using l=.012 mm, this gives a thermal equilibration time of approximately 2 microseconds! This is extremely fast compared to any times required for our experiments and the temperature distribution within the thickness of the sample can be considered to be constant.

The above arguments and agreements between observa-

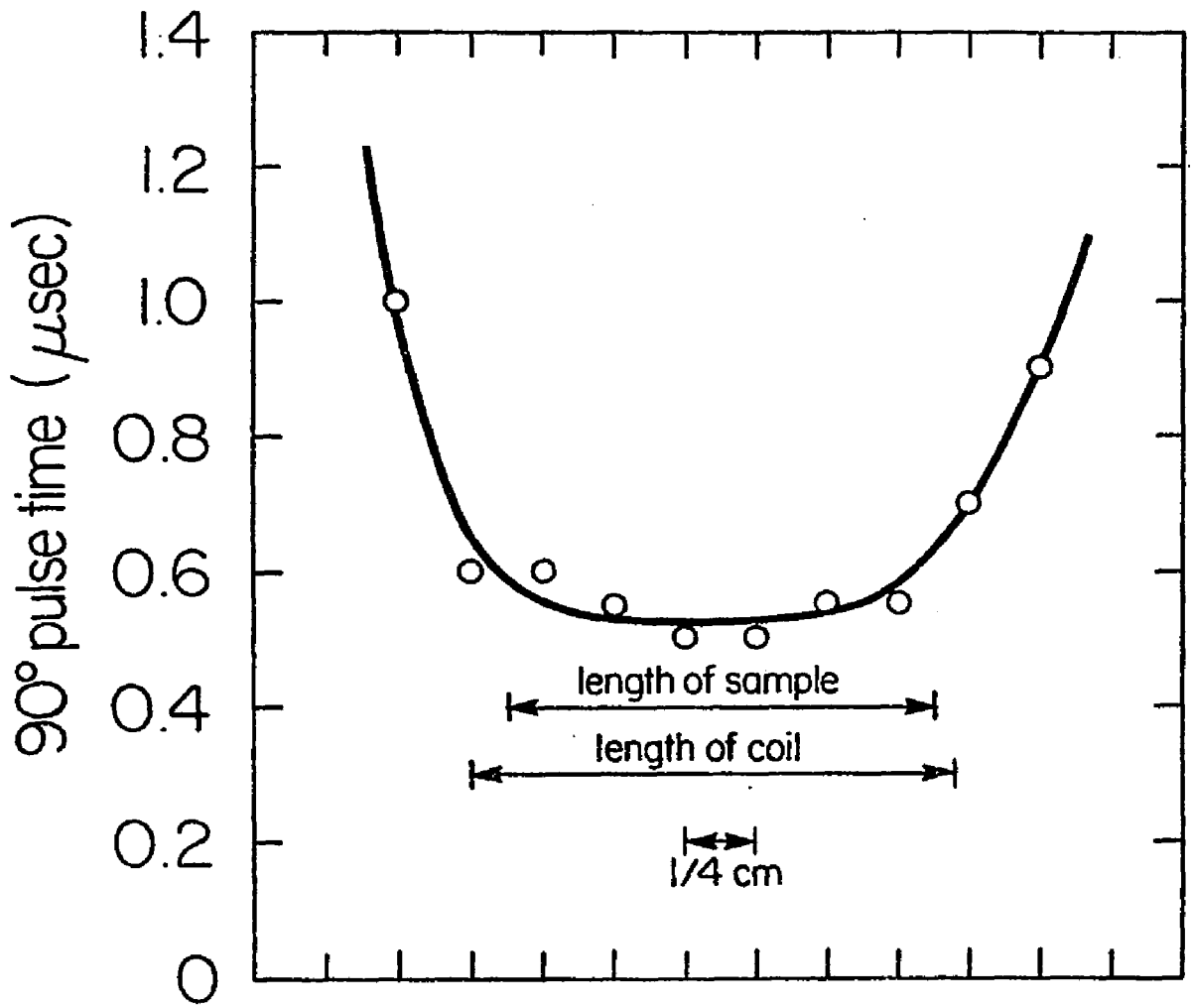

Figure 4.1: H_1 homogeneity of the sample coil.

tion and theory indicate that the observed temperature change is real and that all regions of the sample are at the same temperature.

4.2 ELECTRIC QUADRUPOLE INTERACTION

Since aluminum has spin 5/2, it has an electric quadrupole moment. This can interact with electric field gradients to perturb the nuclear energy levels. Crystals with cubic symmetry have no electric field gradients at the lattice sites provided there exist no imperfections to destroy the symmetry. There are several ways that the quadrupolar interactions can become noticeable in cubic crystals. These are the addition of impurities in high enough concentrations and a high density of crystalline imperfections. Aluminum with 99.9995% purity was used throughout this experiment to eliminate the role of impurities. Vacancies, a major concern here, are a type of imperfection. However, their motion is so fast that any electric field gradients associated with their presence is averaged to zero. This is true provided their concentration is low as is the case in the temperature region of this work (Blo54). It has been noted that the presence of vacancies near the melt has very noticeable effects. The question of other imperfections remains. No direct physical test was performed to detect the presence of

other imperfections. Their absence can be inferred however. Schmidt has noted that the 90° pulse length of the -1/2→1/2 transition for a spin 5/2 nucleus in the presence of quadrupolar interactions is 1/3 the length of a 90° pulse of a spin 5/2 nucleus in the absence of a quadrupole splitting (the rf excites all five transitions in the absence of the quadrupole splitting) (Abr83, Sch72). A simple test along this line was performed to check for the presence of a quadrupolar interaction. A sample of $Al(NO_3)_3$ solution was prepared and NMR was performed on the Al^{+3} ion. In solution, the rapid motion of the ion will average any electric field gradients to zero. Since the aluminum ion and aluminum metal have different frequencies, the spectrometer was tuned to 21.62 Mhz: midway between the two values. The 90° pulse time of the ion was determined and found to be equal to the 90° pulse time of the metal. Thus, the observed metal resonance is from all five degenerate transitions. The quadrupole interaction problem can be safely ignored.

4.3 EQUILIBRIUM DATA

The equilibrium T_{1D} data is presented here. This data allows the determination of the activation energy of diffusion and produces important constants that are needed in the T-jump data. Almost all the data lies

within the temperature range of 510 K to 588 K.

An expression was derived in Chapter II that relates T_{1D} to the jump time and to the relaxation time due to the conduction electrons; it is:

$$1/T_{1D}=2(1-p)/\tau_j+2/T_{1e}. \qquad (4.3)$$

There were remarks made concerning the factor of 2 associated with T_{1e}. To avoid any uncertainty with this factor, it was measured.

The sample was taken to 450 K; here τ_j is so much greater than T_{1e} that the term containing the jump time can be ignored (see Figure 4.2). T_{1D} was measured using the Jeener-Broekaert three pulse sequence: $90_x\text{-}t_w\text{-}45_y\text{-}T^*\text{-}45_y$ (see below). T_{1e} was measured by the pulse sequence diagrammed in Figure 4.3. Signal averaging is used so that for each value of τ the pulse sequence is repeated many times. The long saturation pulse insures that the magnetization is zero immediately after its application; this pulse length was 200 microseconds. τ is the time during which the magnetization recovers and is varied from .01 to .1 seconds. Next comes the 180^o pulse. This pulse is applied only during every other application of the sequence for a given τ for the following reason. When a radiofrequency pulse is applied to a metal, the induced current interacts with the static magnetic field to produce a coherent ultrasonic wave in the metal. During receiv-

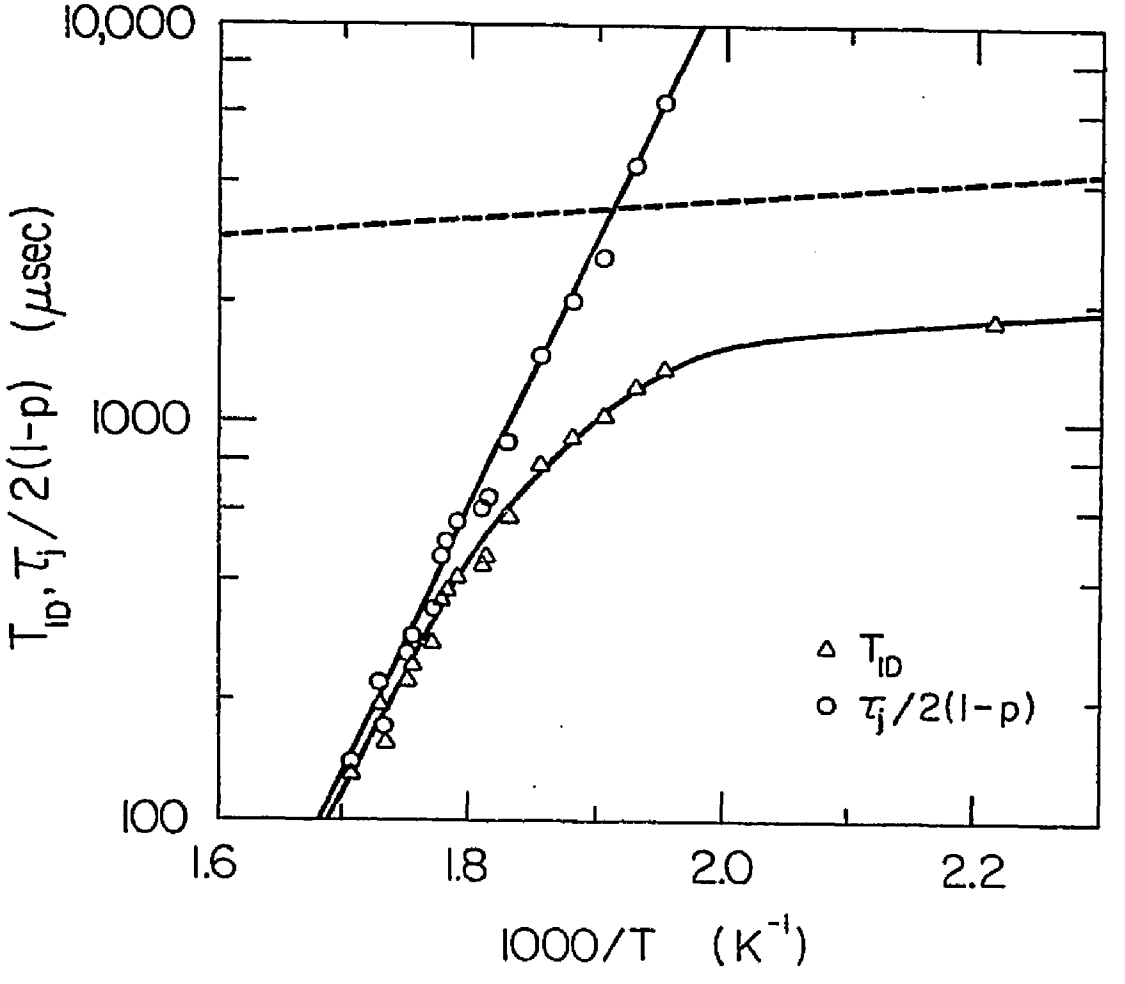

Figure 4.2: Equilibrium T_{1D} and $\tau_j/2(1-p)$ data. The solid line for the T_{1D} data is an eye guide. The line for the jump time data is the best fit and yields E_d=1.33 ev. The dashed line is T_{1e} as determined by $T_{1e}T$=1.802 sec K.

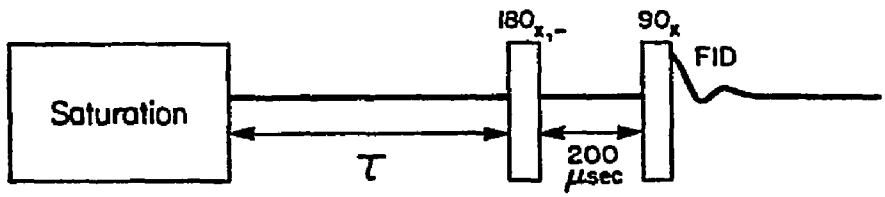

Figure 4.3: T_{1e} pulse sequence.

ing, the acoustic energy is transformed to an oscillating magnetic field which is detected by the probe. This problem is so severe that at many times it can be almost impossible to see a legitimate NMR signal (Bue78, Fuk79). The solution to this problem is to add-subtract the data in such a way that the magnetization adds to a finite value but the spurious signal adds to zero. This is the function of the blinking 180° pulse. Inspection of the magnetization occurs after the 90° pulse. Here the magnetization is inverted on every other application of the pulse sequence by the blinking 180° pulse; the computer multiplies the inverted data by -1 to obtain a finite signal. Since the phase of the spurious signal is determined by the inspection pulse, it is never inverted. The add-subtract manipulation of the data results in the cancellation of the spurious signal. The 200 microsecond period between the 180° and 90° pulses is much less than T_{1e} and has negligible effect on the data; its function is to allow any transverse magnetization to decay before application of the inspection pulse.

The ratio of T_{1e}/T_{1D} was determined to be 2.039. This value will be used instead of the factor of 2 in Equation 4.3, though the difference is negligible.

Instead of measuring T_{1e} at each temperature that T_{1D} was measured, T_{1e} was determined by the relation

$T_{1e}T$=constant. This relation has been described in Chapter II. The T_{1e} data is the same as that used at 450 K and it is found that $T_{1e}T$=1.802 sec K. Using these last two results, Equation 4.3 becomes

$$1/T_{1D}=2(1-p)/\tau_j+(2.039/1.802)T. \qquad (4.4)$$

The equilibrium T_{1D} data was taken using Jeener-Broekaert pulse sequence given above. The pulse lengths and the time t_w were determined by maximizing the Jeener echo at room temperature. These times were determined at room temperature since the signal is much larger than it is at 510 K (Curie's Law). Also, the probe remained tuned when taken from room temperature to 510 K; this implies that the pulse times would be the same at the two temperature regions.

Figure 4.2 shows the equilibrium T_{1D} data. In the cold temperature region of the data (T<510 K), the conduction electrons are the dominant relaxation mechanism. This can be seen by the levelling off of the data. No T_{1D} data is taken when the temperature is greater than 588 K for the following two reasons. First, the T_{1D} times are becoming comparable to T_2 and are difficult to measure (recall that the second pulse occurs during the free induction decay). Second, the strong collision theory of Slichter and Ailion fails whenever the jump time is less than T_2. When this occurs, there is no simple relation relating the jump

time to the dipolar relaxation time. So, there is no need to go higher than 588 K in this work.

Figure 4.2 also shows the jump times calculated from Equation 4.4. The data is remarkably linear. From this line, the activation energy of diffusion is found to be 1.33 ev. This value is in excellent agreement with previous determinations.

4.4 T-JUMP EXPERIMENT

The data of the temperature jump experiment is given here. As mentioned earlier, the idea of this experiment is to change the temperature of the sample from the initial temperature T_i to a final temperature T_f rapidly to create a vacancy concentration out of equilibrium. A measurement of the jump rate as a function of the final temperature will then produce the migration energy.

Figure 4.4 shows the pulse sequence used in this experiment. Recall that the same coil is used for the NMR experiment and for the heating of the sample. The heating pulse was set to have a fixed length of 80 milliseconds. During this 80 milliseconds, the on-off time of the amplifier is adjusted to obtain the desired magnitude of the temperature jump. There is a 20 millisecond wait between the end of the heating pulse and the start of the Jeener-Broekaert pulse sequence.

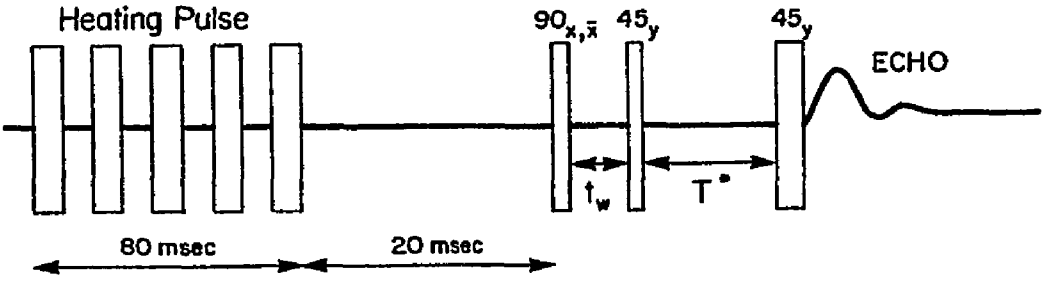

Figure 4.4: Pulse sequence for the T-jump experiment. The last three pulses are the Jeener-Broekaert experiment.

This time is needed for switching the relay. For each value of T^*, 2500 data accumulations were taken. The 90^o pulse was alternately phase shifted by 180^o. This was done so that the acoustic ringing of the sample could be averaged out by operating in the add-subtract mode of data acquisition similar to that described above. The cycle time between each pulse sequence was 3.5 seconds. Typically, six different values of T^* were used for each temperature jump which resulted in a total time of nearly twelve hours for each experiment.

Two T-jump experiments were performed: one with T_i=526 K and one with T_i=542 K. Further experiments with different starting temperatures were considered impractical since the range of useful T_{1D} values occurred over such a small temperature region (510 K to 590 K). Figures 4.5 and 4.6 show $\tau_j/2(1-p)$ as a function of 1000/T for the two starting temperatures. The data with T_i=526 K gave a migration energy equal to .71 ev and the data with T_i=542 K gave E_m=.66 ev. These values are in reasonable agreement with the accepted value given in Chapter II.

The agreement between our experimental value of the migration energy and the accepted value is fortuitous since the heating pulse, as will be seen, may be too long. The mean jump time of an atom can be expressed as

$$\tau_j = C\exp\{E_m/kT_f\}[N/n(T_f)]. \qquad (4.5)$$

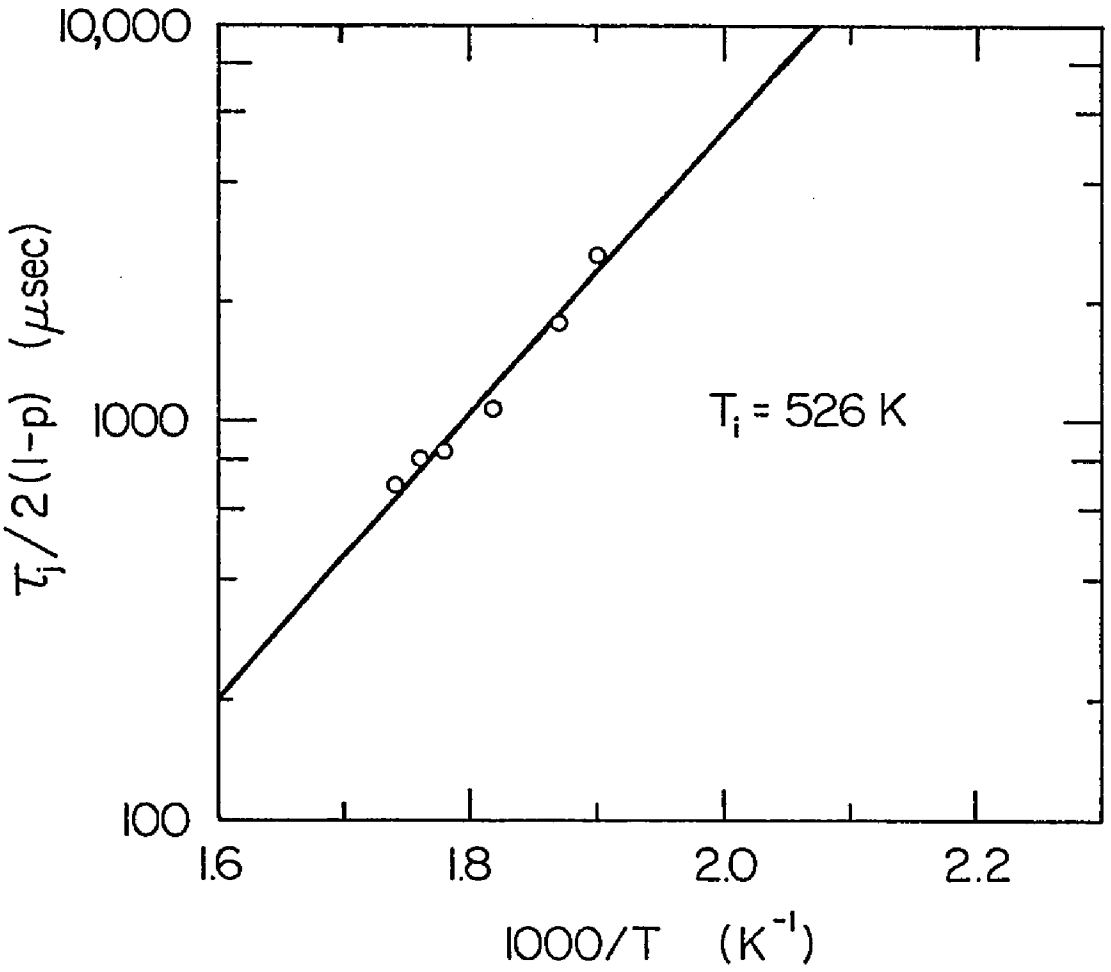

Figure 4.5: T-jump data with T_i=526 K. The line is the best fit and gives E_m=.71 ev.

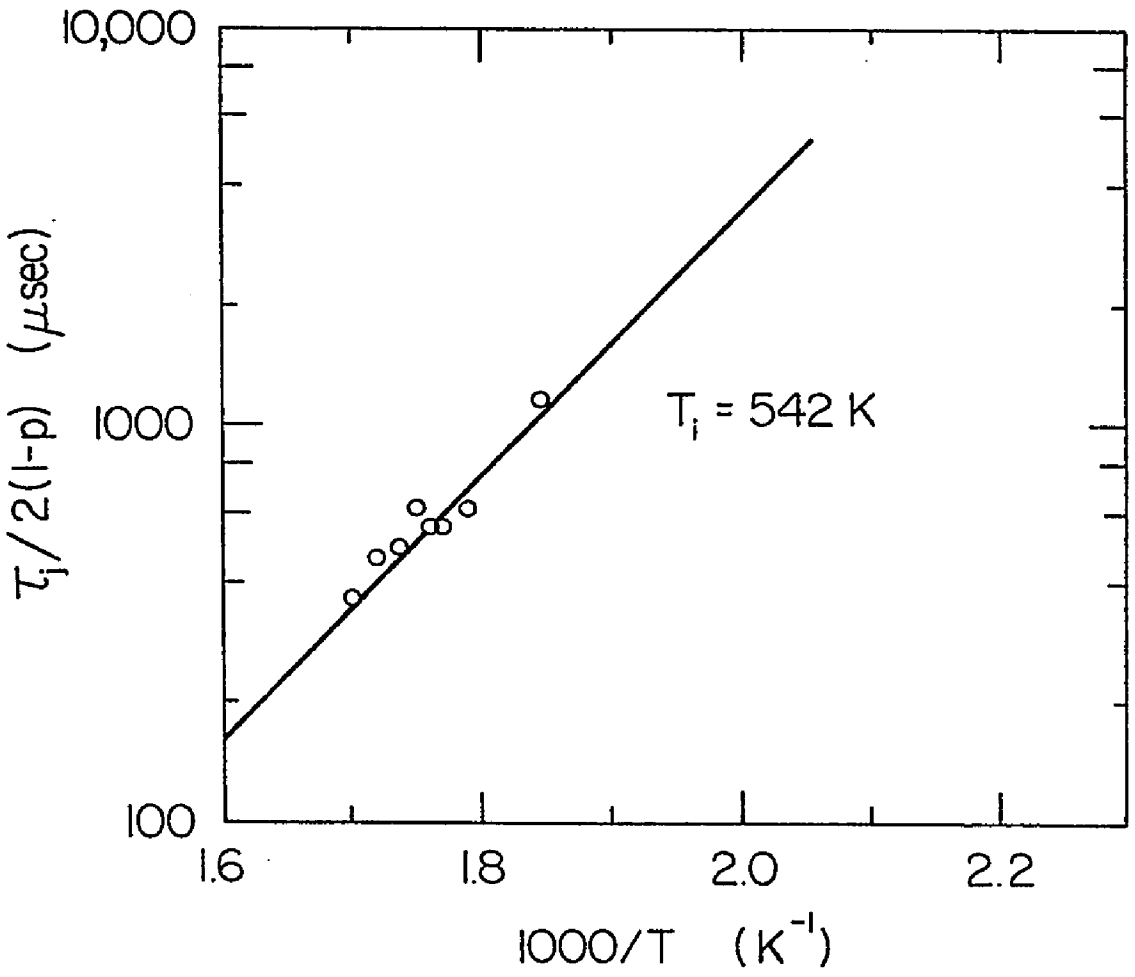

Figure 4.6: T-jump data with T_i=542 K. The line is the best fit and gives E_m=.66 ev.

where $n(T_f)$ is the number of vacancies at the time of the measurement and C is a constant which is independent of temperature. The assumption made was that the heating pulse would be fast enough to ensure that the number of vacancies at T_f would be equal to the equilibrium number of vacancies at T_s: $n(T_f)=n(T_s)$. This assumption was not obeyed during this experiment.

Balluffi and Seidman studied the problem of vacancy recovery in samples which had undergone sudden temperature changes (Bal65, Sei65). An outline of their theory is given in Appendix D. They assumed that the temperature jump was performed instantaneously. Also, they assumed that dislocations are the source of point defects and that these dislocations are arranged as a regular array of straight parallel dislocations. Furthermore, they assumed that each dislocation dominates a cylindrical region with outer radius R and inner radius r_o. They compared the results of their theory to the experimental results in gold. Although their calculated vacancy recovery time was approximately .15 times the observed recovery time, they produced two important results. First, free dislocations and not surfaces are responsible for the generation of vacancies. Second, as expected, the concentration of vacancies begins to recover toward the new equilibrium value immediately after the application of

the heating pulse. These two important results suggest that the vacancy recovery times will be short.

The disagreement between the theory and the experiments of Balluffi and Seidman demonstrate that the determination of the relaxation time of the vacancy concentration must be measured for a given sample. This was not done for aluminum in this lab; fortunately the recovery time for the vacancy concentration in pure aluminum has been measured by Sun. His measurements show that the time needed for the concentration to become equal to the concentration midway between the starting concentration and the final concentration is approximately 200 milliseconds in the temperature region of our experiment. However, this time can only be used as an estimate for our sample since the defects characterizing the two samples will most likely be different. This time is definitely comparable to the 80 milliseconds used to heat the sample in our experiments.

Since our heating pulse was so long, generation of vacancies most likely occurred during the rf heating of the sample. The final concentration of vacancies will be higher than the initial concentration. If the generation of vacancies is thermally activated then, as can be seen from Equation 4.5, the measured "migration energy" will be higher than the actual value.

Although the T-jump data still appear to be

thermally activated, it is highly unlikely that a correction for the additional vacancies can be applied. First, there is no theory that can adequately predict the instantaneous concentration of vacancies. Even the theory of Balluffi and Seidman, which is not too bad, requires knowledge of the density of dislocations and the migration energy. Second, even though Sun has measured the time needed for the relaxation of vacancies in pure aluminum, his relaxation times cannot be used to correct the jump time data obtained here since there will be differences between the samples. Even if both samples were identical, the long heating pulse used here would make correcting for the generation of vacancies nearly impossible. Figure 4.7 shows why. The T-jump occurred over an 80 millisecond time interval and the temperature rose in an almost linear fashion during the first 70 milliseconds. All during the rise in temperature the concentration of vacancies is out of equilibrium, but at the same time the concentration is trying to achieve its equilibrium value. Thus, there is no simple way to use Sun's relaxation times to predict the number of vacancies at the end of our T-jump.

The major problem with the experiment is the slow heating time used. Future work should use much faster heating times. The works of Balluffi and Seidman and of Sun used the method of passing large currents through

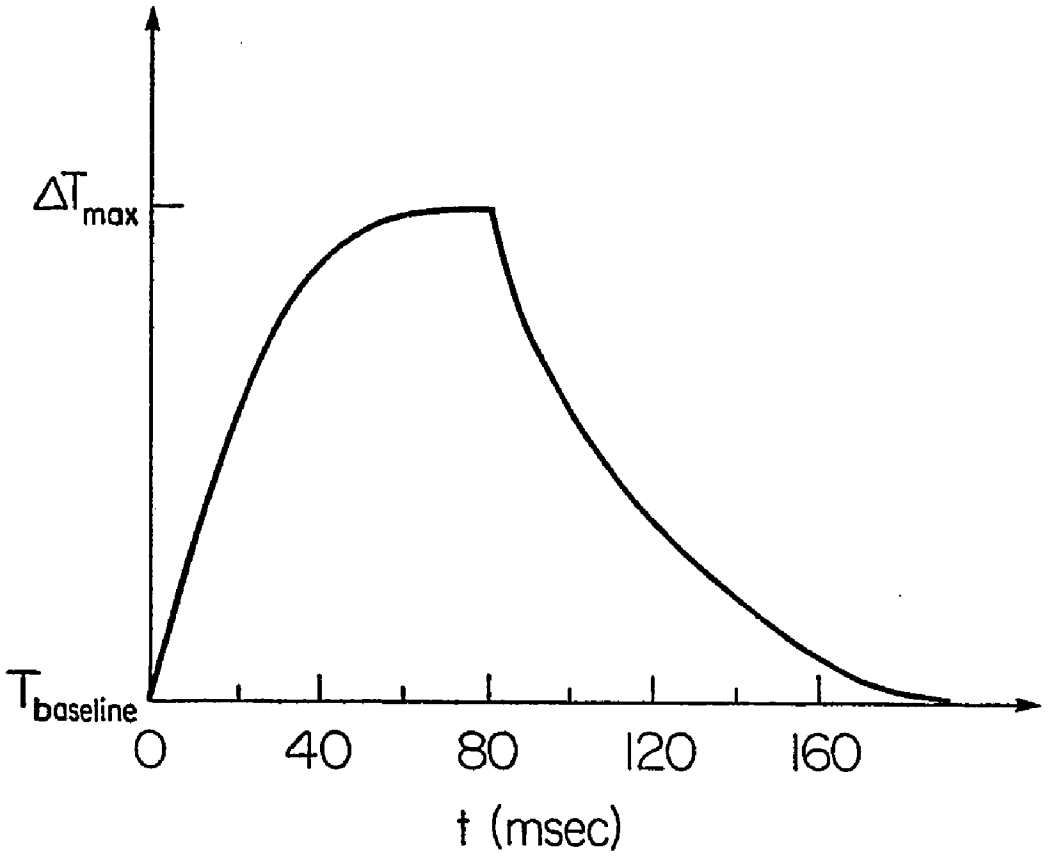

Figure 4.7: Illustration of the temperature response of the sample during the T-jump experiment. The heating pulse is applied during the first 80 msec. The decay time of the temperature is approximately 40 msec.

their samples. Their heating times were 15 milliseconds and 7 milliseconds respectively. Of course, large forces are exerted on the sample because of the coupling between the magnetic field and the current. This puts requirements on supporting the sample and places concerns about the generation of defects during the heating pulse. However, Balluffi and Seidman have shown that their pulsed current heating method did not introduce a noticable number of dislocations in the gold sample. Other methods such as laser heating have been suggested, but this, of course, requires the experiments to be done at large laboratories (and a handful of smaller labs) and , quite frankly, defeats the whole intention of the experiment since it is hoped that the technique will find wide use.

Chapter V

CONCLUSION

A new NMR technique has been demonstrated that provides a means to measure the migration energy, E_m. This NMR experiment is an addition to the class of NMR condition-jump experiments and can be used with most existing pulsed NMR spectrometers.

Although not a goal of this experiment, the activation energy of self diffusion in pure aluminum metal was determined. A value of 1.33 ev was found and is in excellent agreement with past determinations.

The migration energy of pure aluminum was found to be .69 ev (average of the two experiments). This value is only slightly higher than the currently accepted value of .67 ev. This agreement is fortuitous since our heating pulse was rather long. This value should not be considered an accurate determination of the migration energy, but indicates the success and future promise of the T-jump experiment.

Past experiments on aluminum gave vacancy relaxation times near 200 milliseconds (Sun71), but this depends on the dislocation density of the particular

sample. Thus, our sample most likely had a low concentration of dislocations which resulted in a longer vacancy relaxation time; this would minimize the effects of the long heating times used in this work. Unfortunately, no effort was made to check this claim. Future experiments of this sort must take the vacancy relaxation time into consideration and use heating pulses that are very short in comparison.

APPENDIX A

CALCULATION OF THE EQUILIBRIUM CONCENTRATION OF VACANCIES

In this appendix, the equilibrium concentration of vacancies is calculated. The derivation is similar to the one found in the book by Mott and Gurney.

Let the lattice contain N atoms and n vacancies. The energy needed to move an atom from a lattice site within the lattice to the surface of the lattice is called the formation energy and is designated E_f. Thus, the total energy needed to form n vacancies is nE_f. A crystal with N atoms and n vacancies can be arranged P ways; P is given by

$$P=N!/[(N-n)!n!]. \qquad (A.1)$$

The entropy S of a system is defined as the logarithm of the number of states accessible to the system times the Boltzmann factor. Thus, the entropy of a perfect crystal with n vacancies is

$$S=k\ln\{N!/[(N-n)!n!]\}. \qquad (A.2)$$

Using equation A.2 and the energy needed to form n vacancies, the Gibb's function is

$$G=nE_f-kT\ln\{N!/[(N-n)!n!]\} \qquad (A.3)$$

where the PV term has been ignored since it is neg-

ligible at pressures near one atmosphere.

At thermal equilibrium, the free energy must be a minimum with respect to changes in n at constant temperature; that is

$$(\partial G/\partial n)_T=0 \qquad (A.4)$$

Using Stirling's approximation and n<<N, Equation A.4 results in

$$E_f+kT\ln\{n/(N-n)\}=0. \qquad (A.5)$$

This can be written (using n<<N once again) as

$$n/N=\exp\{-E_f/kT\}. \qquad (A.6)$$

n/N is the concentration of vacancies.

APPENDIX B

TEMPERATURE CHANGE AS A FUNCTION OF APPLIED FIELD

When a good conductor is placed in an oscillating magnetic field, the conductor will undergo a change in temperature. This results from joule losses associated with the conduction electrons' response to the applied field. A derivation is given here that relates the change in temperature of the sample as a function of the magnetic field strength. It is assumed that the applied magnetic field intensity is parallel to the surface of the conductor.

The power loss per unit area is

$$dP/da=[\vec{n}X\vec{H}]^2/2\sigma\delta \qquad (B.1)$$

where $\vec{n}$ is a unit vector perpendicular to the sample's surface, H is the magnetic field intensity, σ is the conductivity, and δ is the skin depth. The sample absorbs an amount of heat per unit time according to

$$\Delta Q/\Delta t=mc(\Delta T)/\Delta t \qquad (B.2)$$

where m is the mass of the sample, c is its specific heat, and ΔT is the resulting change in temperature. Since the power loss and the heat absorbed per unit time are the same, the power dissipated per area of sample is

$$P/a=mc(\Delta T)/a\Delta t. \qquad (B.3)$$

Using equations B.1, B.2, and B.3, the temperature change of the sample is

$$\Delta T=H^2\Delta ta/2\sigma\delta mc. \qquad (B.4)$$

The sample of interest in this work has a thickness less than the skin depth. Using this fact and recalling simple relations involving the physical parameters of solids and by recalling that $\vec{B}=\mu\vec{H}$, where $\vec{B}$ is the magnetic induction and μ is the magnetic permeability of free space, Equation B.4 can be written

$$\Delta T=B^2\Delta t/2c\sigma\rho d^2. \qquad (B.5)$$

d is the thickness of the sample and ρ is the density of the sample. The important point is that the change in temperature of the sample is proportional to the length of time the field is applied and to the square of the magnetic induction.

APPENDIX C

CALCULATION OF THE THERMAL EQUILIBRATION TIME

The experiment requires rapid heating of the sample and the measurement of the jump time almost immediately thereafter. An important problem is the uniformity of the temperature throughout the sample when the NMR experiment is performed. Here, the time constant for thermal equilibration t_T is derived.

The heat flow rate between two parts of the sample separated by a small distance l is

$$dQ/dt=kA(\Delta T)/l \qquad (C.1)$$

where k is the thermal conductivity, A is the cross-sectional area, and ΔT is the temperature difference between the two sections of the sample. The exchange of heat per unit time between the two regions also satisfies

$$dQ/dt=mcd(\Delta T)/dt. \qquad (C.2)$$

where m is the mass, and c is the specific heat. The following equation is obtained by equating the above two equations and introducing the density:

$$d(\Delta T)/dt=(k/\rho cl^2)(\Delta T). \qquad (C.3)$$

From this equation, the characteristic time constant t_T

for thermal equilibration is given by

$$t_T=\rho c l^2/k. \qquad (C.4)$$

The l^2 dependence of the time constant shows the necessity of using very thin samples. The density of aluminum is 2.7 gm/cm^3, its specific heat is .91 J/(gm C), and the thermal conductivity is 2.05 J/(sec cm C). These values give

$$t_T=(1.2\ sec/cm^2)l^2. \qquad (C.5)$$

APPENDIX D

THE RECOVERY OF VACANCIES TOWARD EQUILIBRIUM AFTER A SUDDEN CHANGE IN TEMPERATURE

When the temperature of a sample is changed suddenly, the concentration of vacancies is not equal to the equilibrium concentration. There is a finite time required for the vacancy concentration to achieve its equilibrium value. This problem has been studied by Balluffi and Seidman (Bal65, Sei65).

Their model contains the following assumptions and conditions. First, the temperature jump is performed instantaneously from the initial temperature T_i to the final temperature T_f where it remains. Second, dislocations are the source of point defects. Third, the dislocations consist of a regular array of straight parallel dislocations. Fourth, each dislocation dominates a cylindrical region with outer radius R and inner radius r_o. This last assumption implies that the relationship between the outer radius and the dislocation density N_D is

$$R=(\pi N_D)^{-1/2}. \qquad (D.1)$$

The radius of the dislocation core r_o is typically three angstroms.

They solve the general diffusion equation, also known as Fick's Second Law,

$$\partial C/\partial t = V\cdot(DVC) \qquad (D.2)$$

with the following boundary conditions:

$$C(r,0)=0 \qquad r_o<r<R \qquad (D.3)$$

$$C(r_o,t)=C_o \qquad \text{all } t \qquad (D.4)$$

$$(\partial C/\partial r)_{r=R}=0 \qquad \text{all } t. \qquad (D.5)$$

C_o is the equilibrium concentration at T_f and D is the defect diffusivity. The solution to D.2 is

$$[C_o-C(t)]/C_o=\exp\{-2\pi N_D Dt/\ln(R/r_o)\}. \qquad (D.6)$$

It is important to keep in mind that the defect diffusivity is thermally actived. C(t) is the average concentration of the entire cylinder as a function of time.

Seidman and Balluffi performed T-jump experiments on pure gold. The vacancy concentration was determined by resistivity measurements. Their calculated vacancy generation rate was approximately $(.15)^{-1}$ the rate measured in gold. Considering their assumptions for the distribution of dislocations, their theory is not a total failure. They were still able to deduce that free surfaces are not responsible for vacancy generation by solving Equation D.2 and using boundary conditions suitable for a thin slab.

REFERENCES

Abr83 A. Abragam, The Principles of Nuclear Magnetism, Oxford (1983).

Ail71 D. C. Ailion, Advances in Magnetic Resonance, Vol. 5, edited by J. S. Waugh, Academic Press (1971).

And59 A. G. Anderson and A. G. Redfield, Phys. Rev., 116, 583 (1959).

And62 A. G. Anderson and S. R. Hartmann, Phys. Rev., 128, 2023 (1962).

Bal65 R. W. Balluffi and D. N. Seidman, J. Appl. Phys., 36, 2708 (1965).

Bas67 J. Bass, Phil. Mag., 15, 717 (1967).

Bey68 M. Beyeler and Y. Adda, J. Phys., 29, 345 (1968).

Bia66 G. Bianchi, D. Mallefac, C. Janot, and G. Champier, Comp. Rend., 263, 1404 (1966).

Blo48 N. Bloembergen, E. M. Purcell, and R. V. Pound, Phys. Rev. 73, 679 (1948).

Blo54 N. Bloembergen, in Report of the Conference on Defects in Crystalline Solids, 1954 (Physical Society, London, 1954).

Bou68 R. R. Bourassa, D. Lazarus, and D. A. Blackburn, Phys. Rev., 165, 853 (1968).

Bue78 M. L. Buess and G. L. Peterson, Rev. Sci. Inst., 49, 1151 (1978).

Cer63 S. Ceresara, T. Federighi, and D. Gelli, Nuovo Cimento, 29, 1244 (1963).

Cro76 V. R. Cross, R. K. Hester, and J. S. Waugh, Rev. Sci. Instr., 47, 1486 (1976).

Des59a W. Desorbo and D. Turnbull, Acta. Meta.,7, 83 (1959).

DeS59b W. DeSorbo and D. Turnbull, Phys. Rev., 115, 560 (1959).

Dlu77 G. Dlubek, O. Brummer, and N. Meyendorf, Phys. Status Solidi (a), 29, K95 (1977).

Duc66 F. C. Duckworth and J. Burke, Phil. Mag., 14, 473 (1966).

Fed58 R. Feder and A. S. Nowick, Phys. Rev., 109, 1959 (1958).

Fed59 T. Federighi, Phil. Mag., 4, 502 (1959).

Fed65 T. Federighi, Lattice Defects in Quenched Metals, edited by R. M. J. Cotterill, M. Doyoma, J. J. Jackson, and M. Meshii, Academic Press (1965).

Flu78 M. J. Fluss, L. C. Smedskjaer, M. K. Chason, D. G. Legnini, and R. W. Siegel, Phys. Rev. B, 17, 3444 (1978).

Fra67 F. Y. Fradin and T. J. Rowland, Appl. Phys. Lett., 11, 207 (1967).

Fuk79 E. Fukushima and S. B. W. Roeder, J. Magn. Res., 33, 199 (1979).

Fuk81 E. Fukushima and S. B. W. Roeder, Experimental Pulse NMR: A Nuts and Bolts Approach, Addison-Wesley Publishing Company, Inc. (1981).

Fur76 K. Furukawa, J. Takamura, and N. Kuwana, J. Phys. Soc. Japan, 41, 1584 (1976).

Gul84 T. Gullion and M. S. Conradi, Phys. Rev. B, 30, 1133 (1984). Hal74

Gul85 T. Gullion and M. S. Conradi, Phys. Rev. B, 32, 7076 (1985).

Hah50 E. L. Hahn, Phys. Rev., 80, 580 (1950).

Hal74 T. M. Hall, A. N. Goland, and C. L. Snead, Phys. Rev. B, 10, 3062 (1974).

Har72 E. A. Harrison and P. Wilkes, J. Phys. E, 5, 174 (1972).

Has80 E. Hashimoto, Y. Murakami, and T. Kino, J. Phys. Soc. Japan, 49, 1123 (1980).

Hau79 P. Hautojarvi and A. Vehanen, Positrons in Solids, edited by P. Hautojarvi, Springer-Verlag (1979).

Jee67 J. Jeener and P. Broekaert, Phys. Rev., 157, 232 (1967).

Kab65 S. Kabemoto, Japan. J. Appl. Phys., 4, 896 (1965).

Kan80 S. Kan, M. Fan, and J. Courtieu, Rev. Sci. Instrum., 51, 887 (1980).

Kim74a S. M. Kim and W. J. L. Buyers, Phys. Lett., 49A, 181 (1974).

Kim74b S. M. Kim, W. J. L. Buyers, P. Martel, and G. M. Hood, J. Phys. F, 4, 343 (1974).

Kni56 W. D. Knight, Solid State Physics, Vol. 2, edited by F. Seitz, D. Turnbull, and H. Ehrenreich, Academic Press (1956).

Kor50 J. Korringa, Physica, 16, 601 (1950).

Kuh82 P. Kuhns, Ph. D. Thesis, The College of William and Mary (1982).

Liu84 S-B. Liu and M. S. Conradi, Phys. Rev. B, 30, 24 (1984).

Lun62 T. S. Lundy and J. F. Murdock, J. Appl. Phys., 33, 1671 (1962).

McK72 B. T. A. McKee, W. Triftshauser, and A. T. Stewart, Phys. Rev. Lett., 28, 358 (1972).

Mer70 E. Merzbacher, Quantum Mechanics, Second Ed., John Wiley and Sons (1970).

Mot64 N. F. Mott and R. W. Gurney, Electronic Processes in Ionic Crystals, Second Ed., Dover Publications, Inc. (1964).

Ono78 K. Ono and T. Kino, J. Phys. Soc. Japan, 44, 875 (1978).

Pan58 C. Panseri and T. Federighi, Phil. Mag., 3, 1223 (1958).

Pet68 N. L. Peterson, Solid State Physics, Vol. 22, edited by F. Seitz, D. Turnbull, and H. Ehrenreich, Academic Press (1968).

Red55 A. Redfield, Phys. Rev., 98, 1787 (1955).

Rei65 F. Reif, Fundamentals of Statistical and Thermal Physics, McGraw-Hill Book Co. (1965).

Sch72 V. H. Schmidt, Pulsed Magnetic and Optical Resonance, Proceedings of the Ampere International Summer School II, edited by R. Blinc (1972).

See73 A. Seegar, J. Phys. F, 3, 248 (1973).

Sei65 D. N. Seidman and R. W. Balluffi, Phys. Rev., 139, 1824 (1965).

Sen71 R. E. Sentz, Modern Communications Electronics, Rinehart Press (1971).

She63 P. G. Shewmon, Diffusion in Solids, McGraw-Hill Book Company, Inc. (1963).

She79 J. N. Sherwood, The Plastically Crystalline State, edited by J. N. Sherwood, John Wiley and Sons (1979).

Sim60a R. O. Simmons and R. W. Balluffi, Phys. Rev., 117 , 52 (1960).

Sim60b R. O. Simmons and R. W. Balluffi, Phys. Rev., 117, 62 (1960).

Sli80 C. P. Slichter, Principles of Magnetic Resonance, Springer-Verlag (1980).

Sli64 C. P. Slichter and D. Ailion, Phys. Rev., 135, 1099 (1964).

Sne72 C. L. Snead, T. M. Hall, and A. N. Goland, Phys. Rev. Lett., 29, 62 (1972).

Spo59 J. J. Spokas and C. Slichter, Phys. Rev., 113, 1462 (1959).

Sto65 T. G. Stoebe, R. D. Gulliver II, T. O. Ogurtana, and R. A. Huggins, Acta Meta., 13, 701 (1965).

Sun71 C-Y. Sun, Ph. D. Thesis, U. of Illinois (1971).

Tak65 J. Takamura, Lattice Defects in Quenched Metals, edited by R. M. J. Cotterill, M. Doyama, J. J. Jackson, and M. Meshii, Academic Press (1965).

Tri75 W. Trifthauser, Phys. Rev. B, 12 4634 (1975).

Tza76 P. Tzanetakis, J. Hillairet, and G. Revel, Phys. Stat. Sol. (b), 75, 433 (1976).

Van66 J. T. Vanderslice, H. W. Schamp Jr., and E. A. Mason, Thermodynamics, Prentice-Hall, Inc. (1966).

Wes79 R. N. West, Positrons in Solids, edited by P. Hantojarvi, Springer-Verlag (1979).

Win71 J. Winter, Magnetic Resonance in Metals, Oxford (1971).

VITA

TERRY WILLIAM GULLION

The author was born in Princeton, West Virginia on March 12, 1958. He received a B.S. degree (June, 1981) from Western Carolina University; he received his M.S. degree (December, 1982) and his Ph.D. degree (October, 1986) from The College of William and Mary. He accepted a postdoctoral position at the chemistry department of Washington University.